



# **Solar wind forcing of the high-latitude ionosphere-thermosphere (IT) system**

**CEDAR Distinguished Lecture**

**20 June 2019**

**Cheryl Huang**

**Air Force Research Laboratory**

**Space Vehicles Directorate**

**Thanks to many who contributed to this talk -**

**Collaborators:**

Yanshi Huang (HIT)

Yi-Jiun Su (AFRL)

Russell Landry (UNM)

Vince Eccles (SDL)

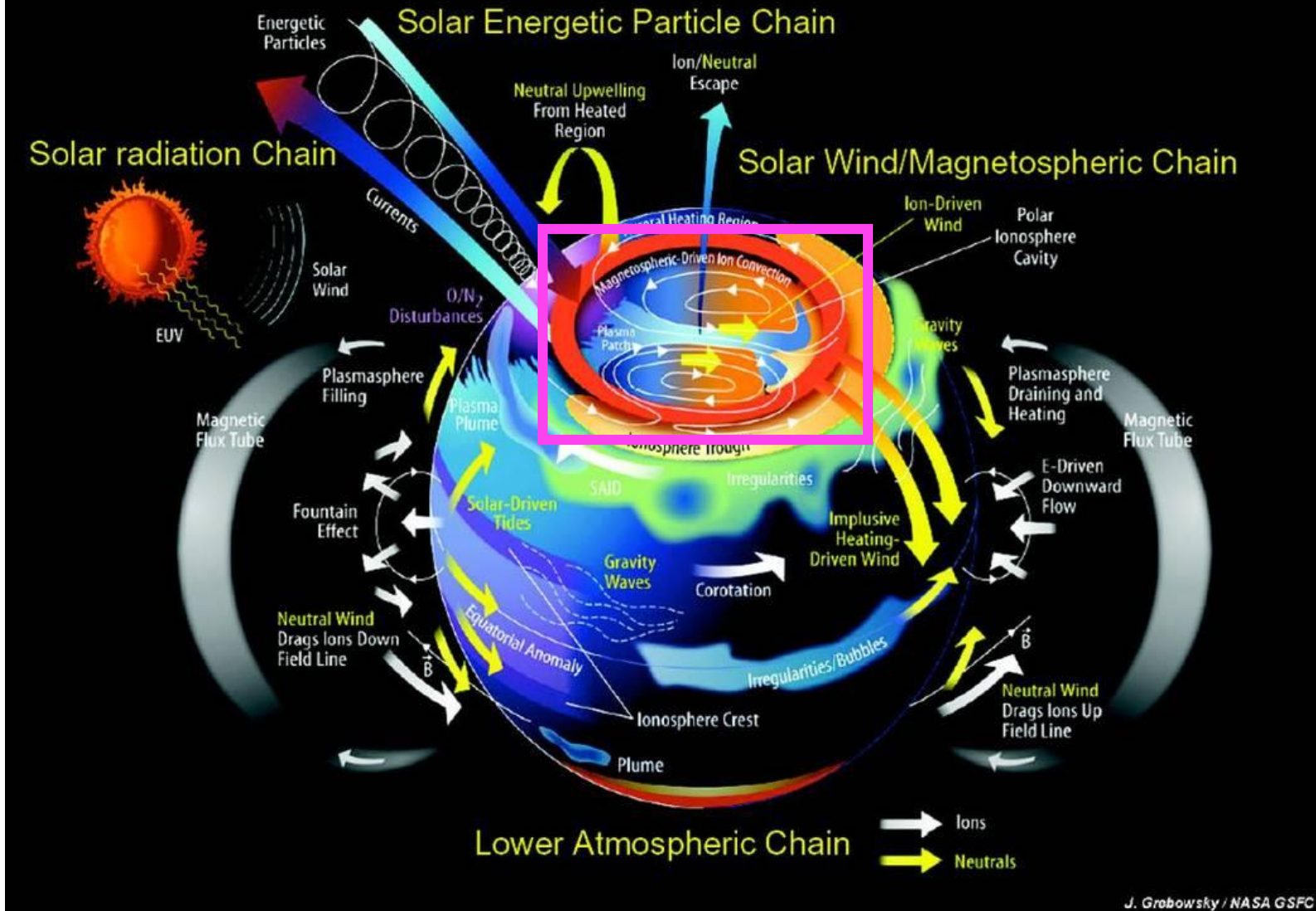
Jeff Holmes (AFRL)

and many more for stimulating exchanges over the years....

**Support:**

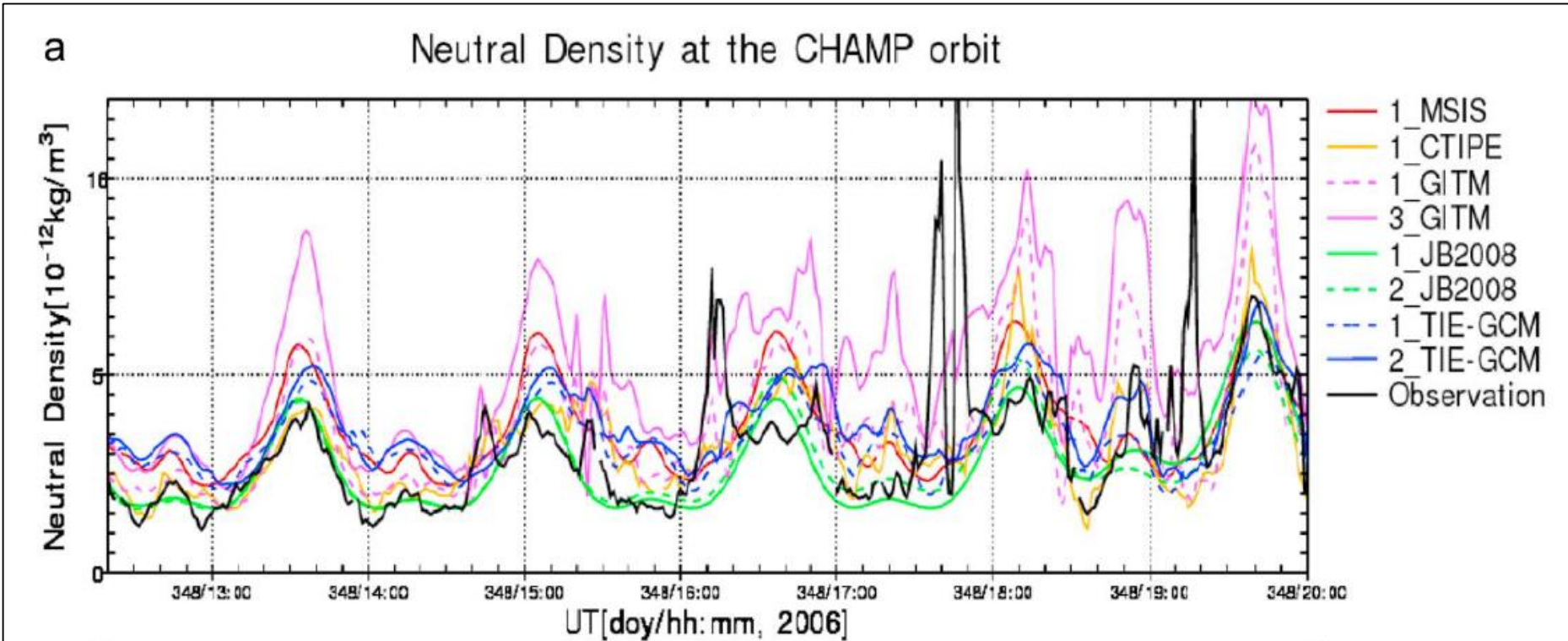
AFOSR Space Sciences (Julie Moses, Kent Miller)

# Terrestrial Atmosphere ITM Processes



For DoD, accurate *specification* and *forecast* of the space environment are critical.

Currently most operational models used by DoD for the IT system are empirical, with and without data assimilation.



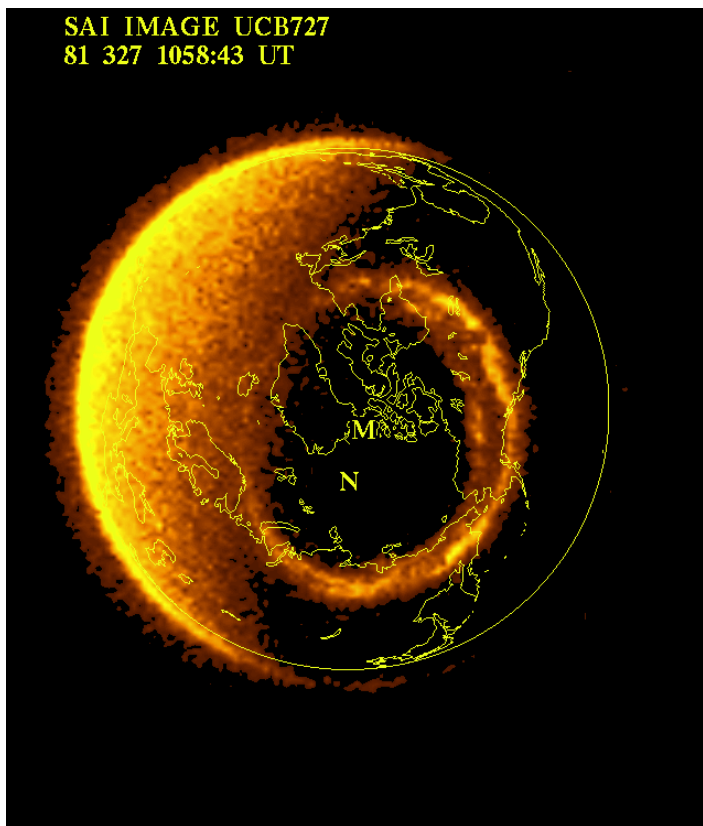
[Shim et al., 2012]

What is lacking in physics-based models, and what can be done to improve specification and forecast?

Assumption: Physics in the models is correct, and problem is in the external driver specification.

## Outline:

- Introduction
- Physics-based models
  - Solar wind drivers
- Observations of energy input
  - Poynting flux and Joule heat
- Observations of energy dissipation
  - Particle precipitation and conductance
  - Heating of neutrals
- Outstanding challenges
  - Scale sizes, variability
  - Geoeffectiveness



NH aurora observed by DE-1 satellite,  
[<http://www-pi.physics.uiowa.edu/sai/gallery/>]

The paradigm for energy entry/dissipation is based on energetic particle precipitation leading to auroral emissions.

This paradigm has been broken!

Electromagnetic energy is the dominant form of energy input to the ionosphere [Knipp et al., 2005, Huang et al., 2014]. Estimated ratio of electromagnetic/particle energy ranges from 2-10.

However particle precipitation leads to conductivity which determines energy dissipation

## Outline:

- Introduction
- **Physics-based models**
  - **Solar wind drivers**
- Observations of energy input
  - Poynting flux and Joule heat
- Observations of energy dissipation
  - Particle precipitation and conductance
  - Heating of neutrals
- Outstanding challenges
  - Scale sizes, variability
  - Geoeffectiveness



The most widely used physics-based models in IT are the General Circulation Models (GCMs). They solve the momentum, continuity and energy equations for ions, electrons and (sometimes) neutrals. They include solar radiation, transport, chemistry....

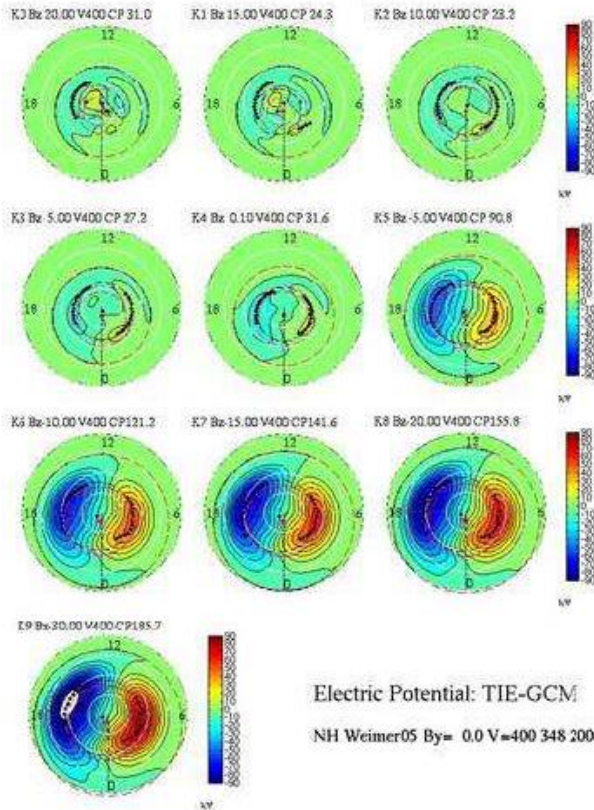
What they do not contain are the high-latitude electric field (energy into IT) and the conductivity (energy dissipation in IT) due to the solar wind. These are referred to as the drivers. They have to be provided.

The drivers are usually given by empirical or assimilative models, or coupling to a magnetospheric model. The IT system comes to equilibrium with the drivers. Note that the drivers must be specified for the entire high-latitude region.

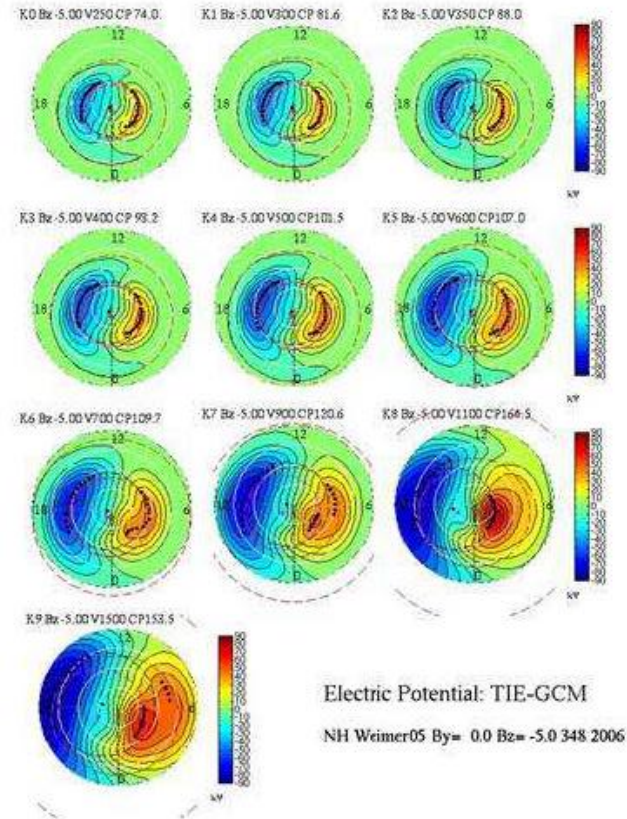
Widely used drivers are the empirical models Weimer (2005) for high-latitude electric field, and the Roble and Ridley (1987) model for conductivity.



# Weimer 2005 NH By=0

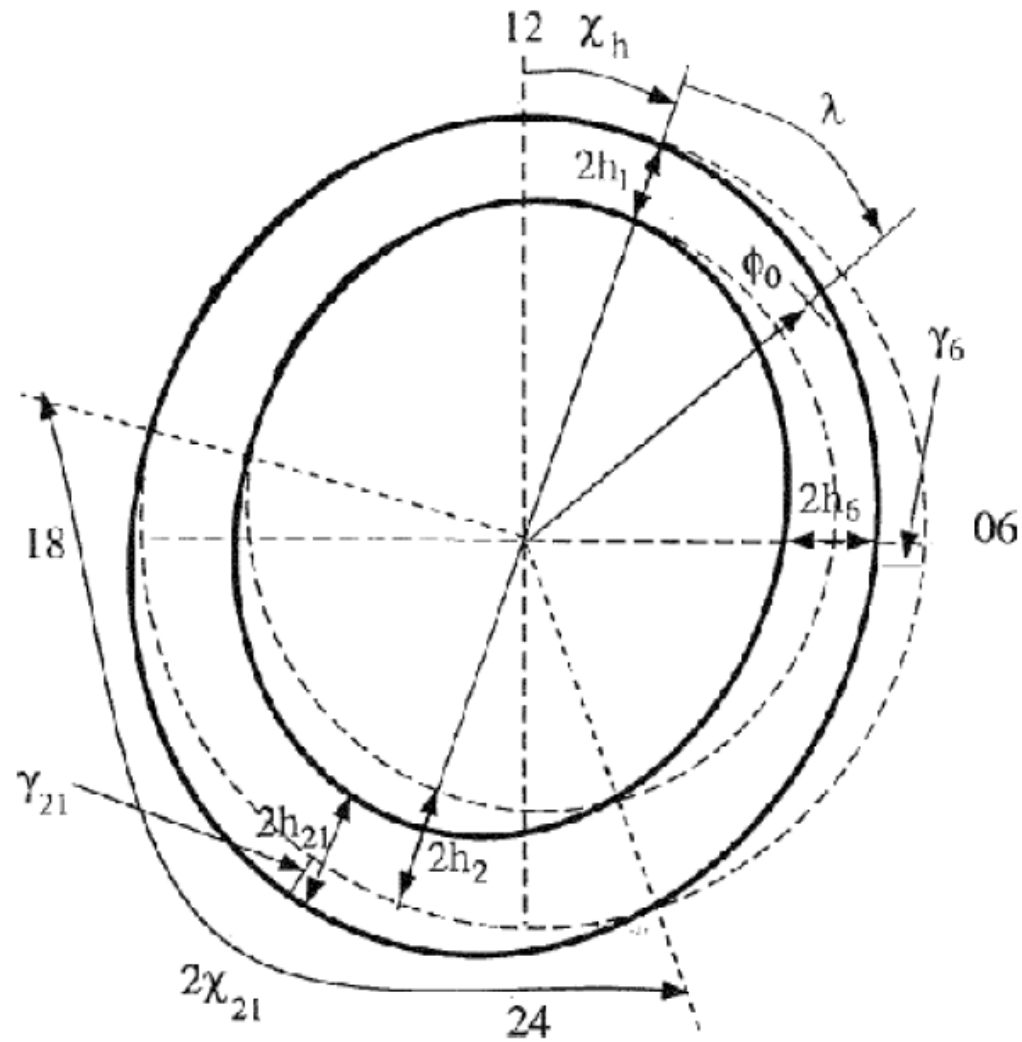


Vsw=400 km/s, Bz=+20 to -30 nT

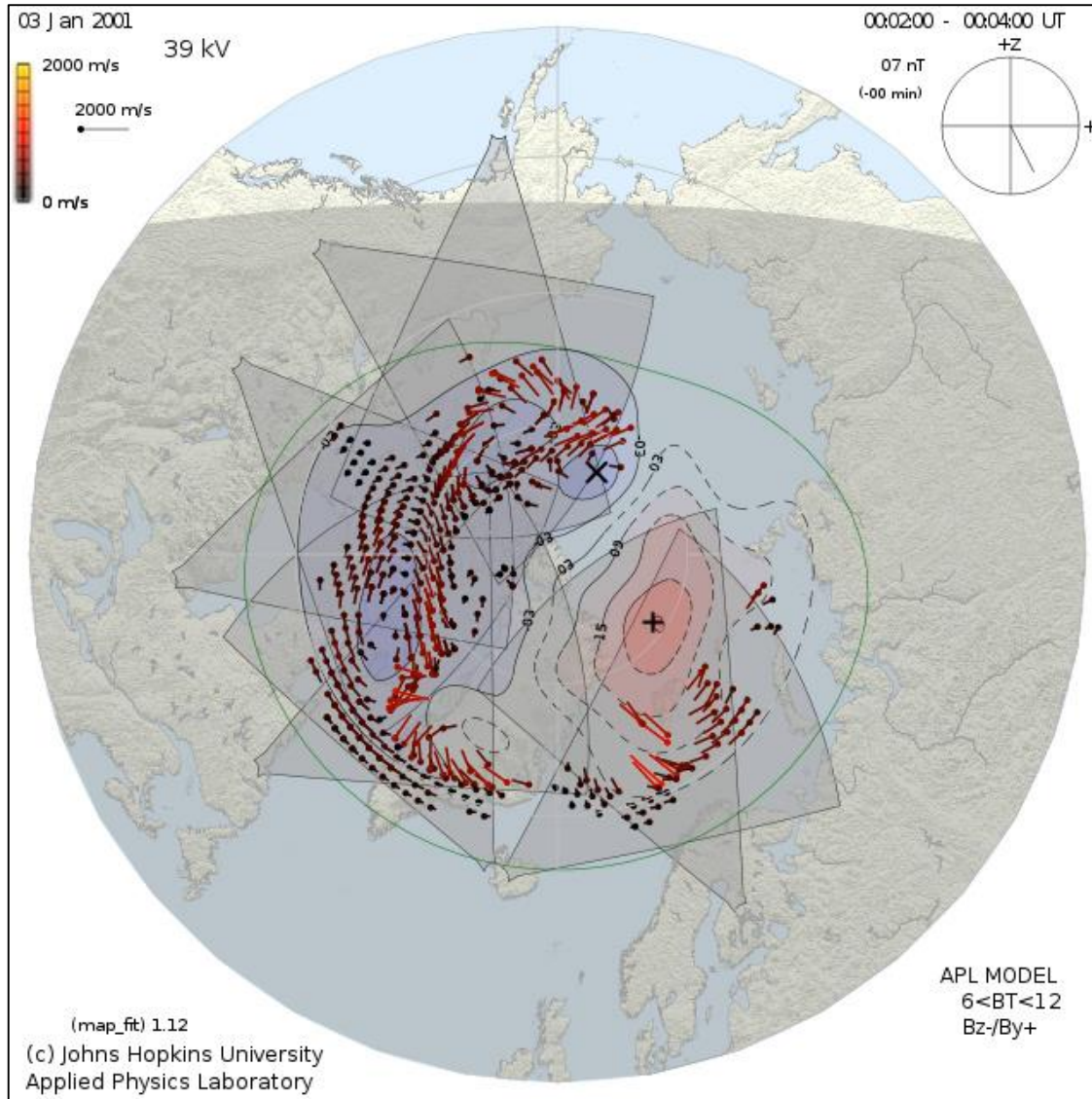


Bz=-5, Vsw=250 to 1500 km/s

[TIEGCM Handbook, 2016]



[TIEGCM Handbook, 2016]



Dynamics in ionospheric observations are not captured by smooth, averaged empirical models.

Even when the cross-polar cap potential is low, there are dynamic electric fields.

[Acknowledgments  
APL:Jesper Gjerloev,  
Robin Barnes, Ethan  
Miller;  
SuperDARN community]

## Outline:

- Introduction
- Physics-based models
  - Solar wind drivers
- **Observations of energy input**
  - **Poynting flux and Joule heat**
- Observations of energy dissipation
  - Particle precipitation and conductance
  - Heating of neutrals
- Outstanding challenges
  - Scale sizes, variability
  - Geoeffectiveness

Observed energy into the system:

Poynting Flux:

Use measured convection measured at DMSP (operational satellite system, orbital altitude 840 km, sun-synchronous orbits at 97° inclination) to calculate the convective electric field,  $E = -v \times B$ .

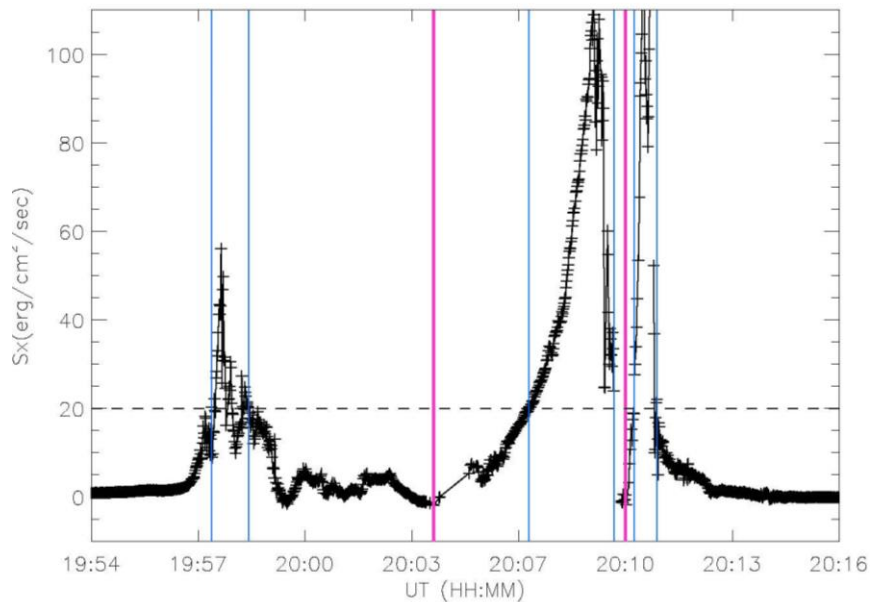
Use perturbation magnetic fields,  $\delta B$ , measured at DMSP, to compute Poynting flux (PF), the energy per unit time entering the IT system.

$$S (mW m^{-2}) = \frac{E \times \delta B}{\mu_0}$$

The coordinate system used defines  $S$  as positive for downward-directed Poynting flux, i.e. power *into* the IT system [Kelley et al., 1991; Huang and Burke, 2005]. We use the cross-track velocities in our PF estimates.

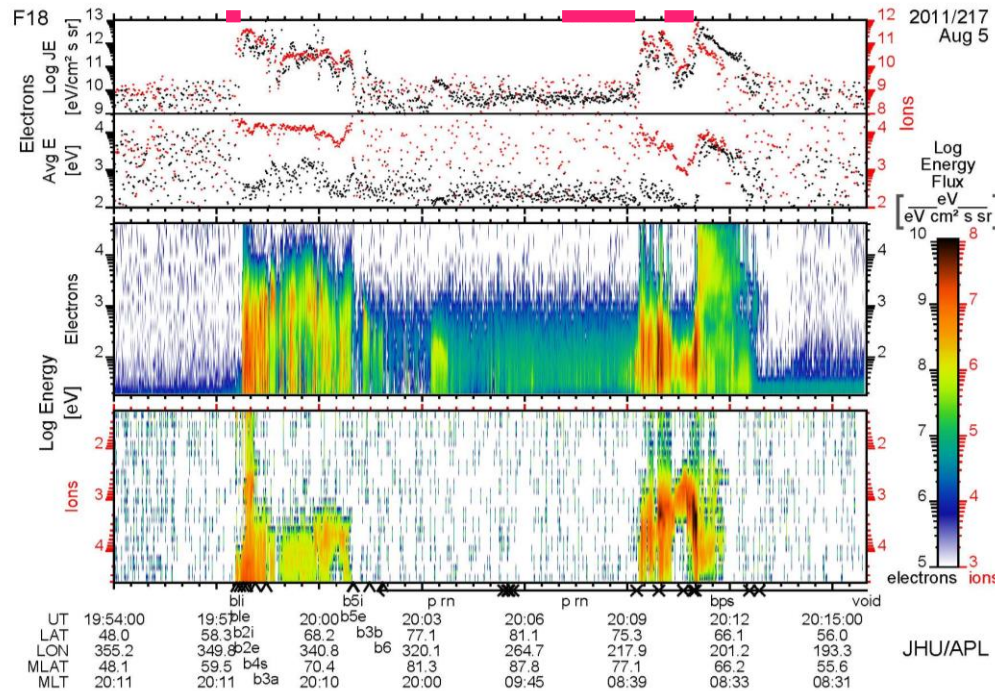
Poynting's theorem defines Joule heat ( $\sigma_p E^2$ ) as the *divergence* of PF. Joule heat and PF are not identical [Richmond, 2010].





## Example: DMSP Poynting flux and particle precipitation

Poynting flux (top) and particle precipitation (bottom) measured by DMSP F18 during magnetic storm on 5-6 August 2011.

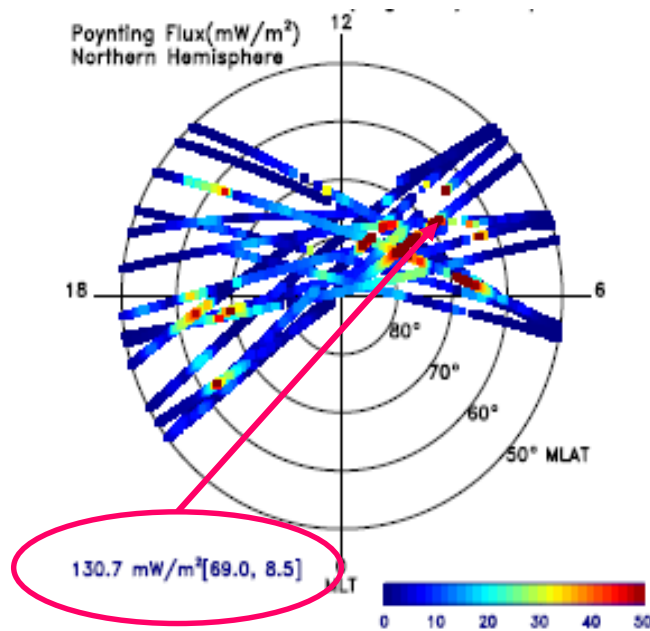


Magenta vertical lines indicate polar cap boundaries. Blue vertical lines indicate regions when PF > 20 mW m<sup>-2</sup>.

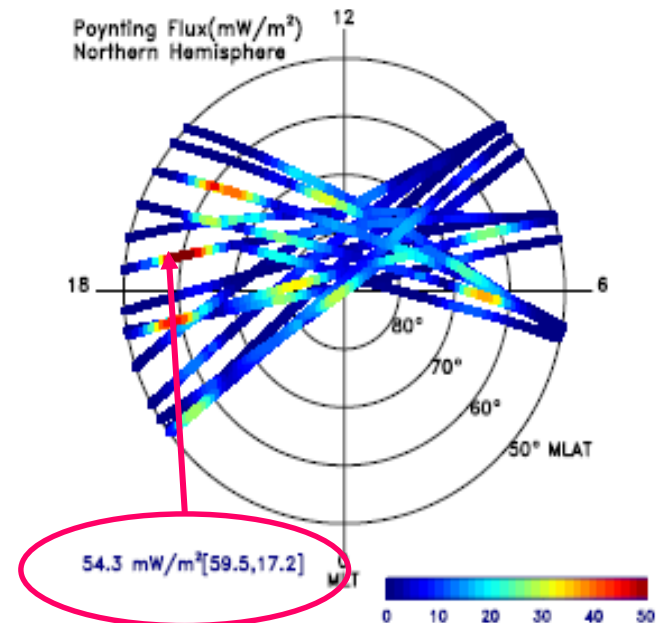
Regions of high PF (> 20 mW m<sup>-2</sup>), with corresponding boundary IDs shown below by heavy magenta bars.

Comparison of observed PF with empirical model (Weimer, 2005) for magnetic storm storm

Observed Poynting flux from DMSP for magnetic storm on 5 August 2011



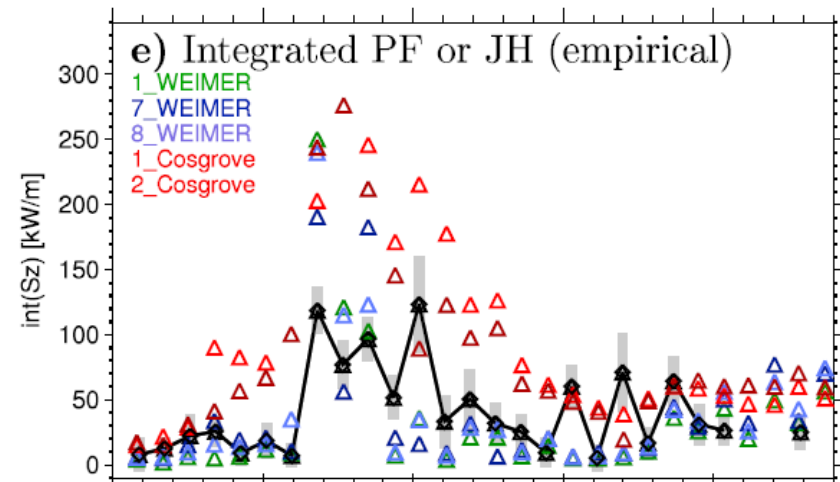
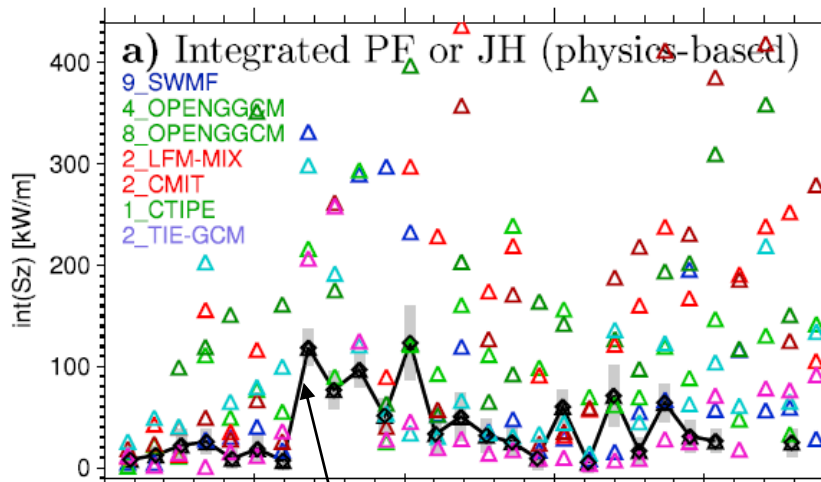
Predicted Poynting flux along DMSP orbit (Weimer model)



Detailed magnitudes and spatial distribution of PF entry are not captured well for individual events by empirical models [Huang et al., 2017].



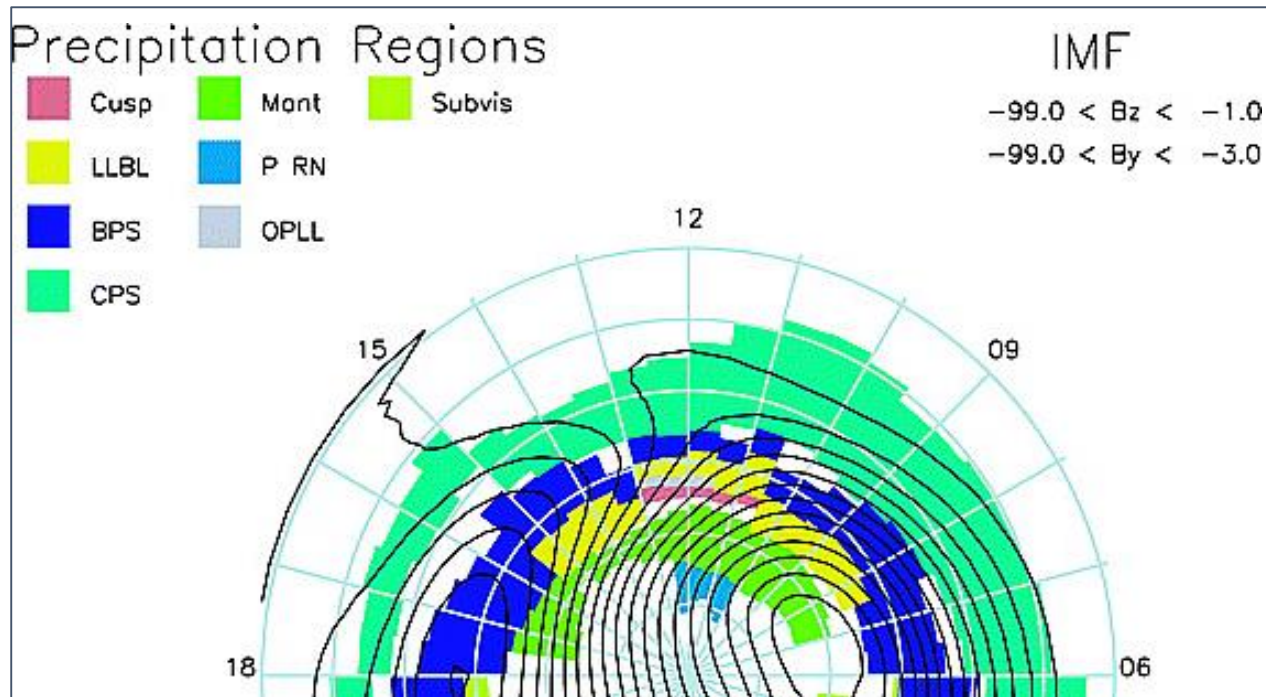
Model comparison: Observed Poynting flux at DMSP and modeled Joule heat [Rastätter et al., 2016] showing discrepancies between observations and model specifications.



Observations (DMSP F15)

## Outline:

- Introduction
- Physics-based models
  - Solar wind drivers
- Observations of energy input
  - Poynting flux and Joule heat
- **Observations of energy dissipation**
  - **Particle precipitation and conductance**
  - **Heating of neutrals**
- Outstanding challenges
  - Scale sizes, variability
  - Geoeffectiveness

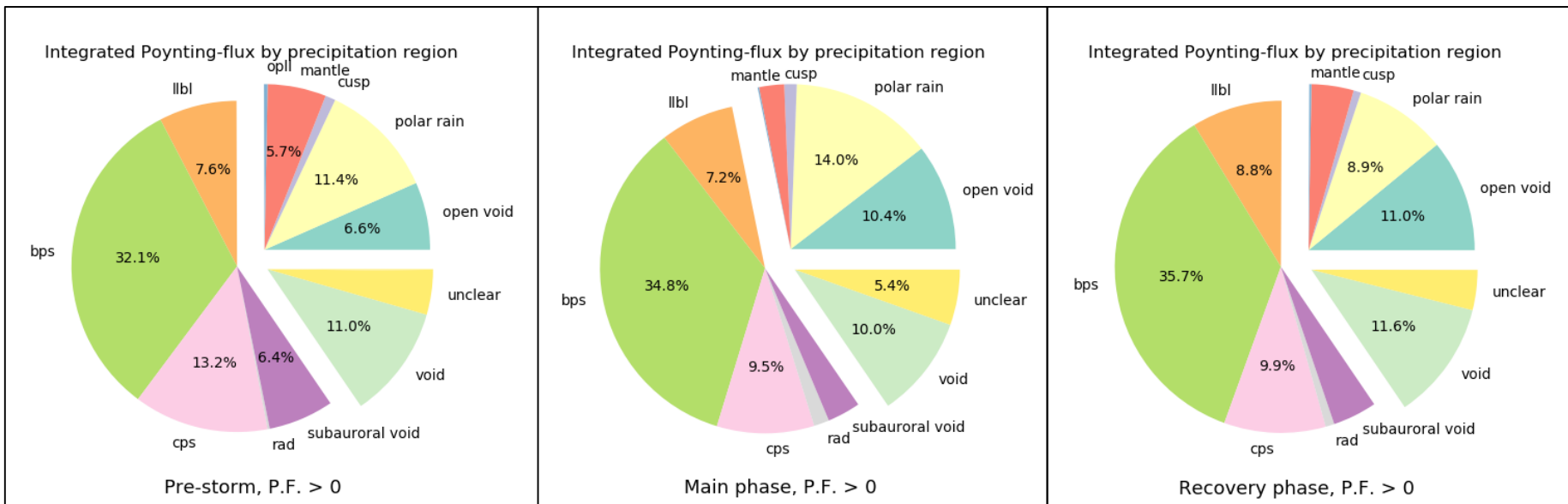


[Newell et al., 2005]

Data selection: Database of 44 magnetic storms, from 2001 to 2012. Divide storms into pre-storm quiet, main phase, recovery.

Restrict observations to dayside, NH passes. Use the APL DMSP tool to define boundaries. Sort PF, particle data into regions based on Newell definitions.

Integrating PF along DMSP orbits, and dividing results into precipitation regions shows:



## Conclusions:

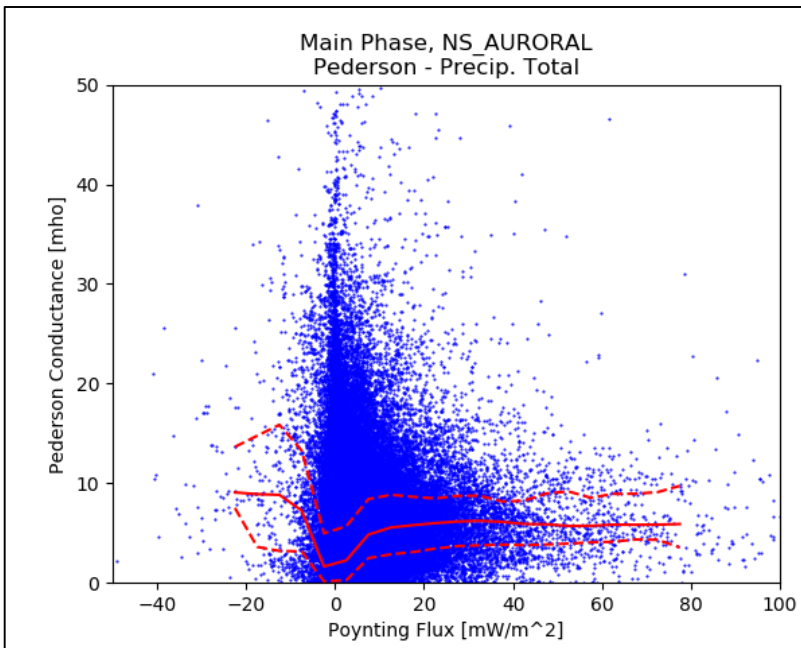
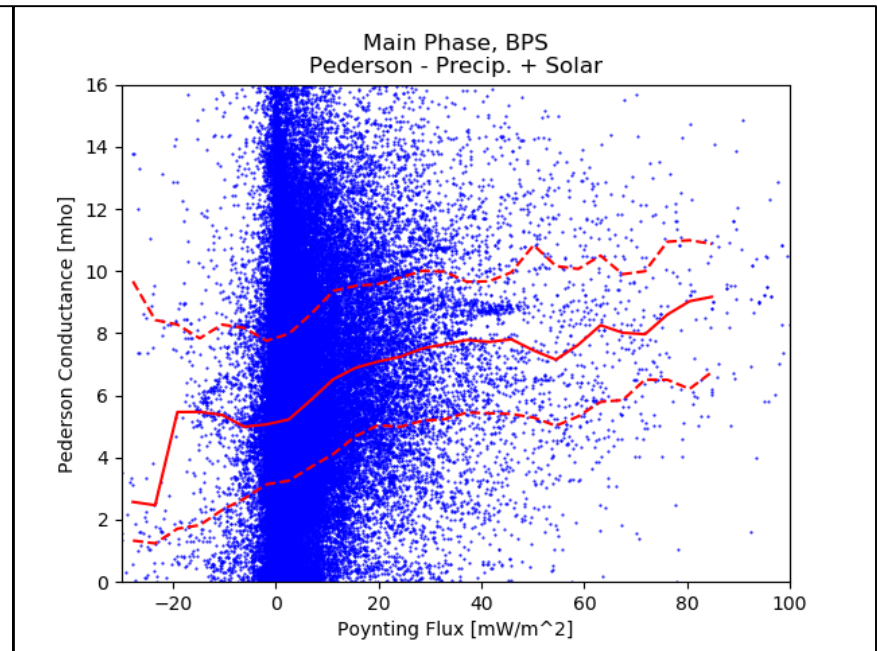
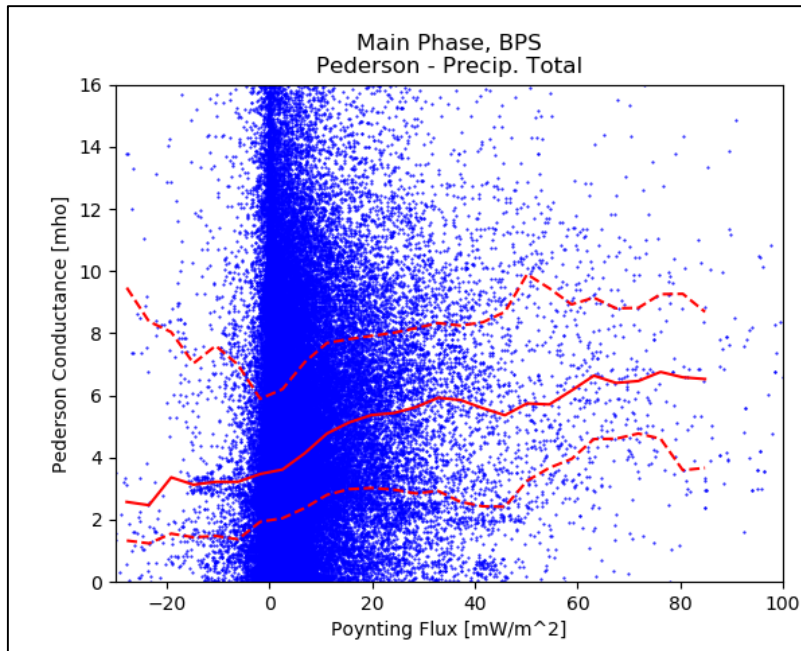
For 44 storms, a total of 1726 hours of satellite data were analyzed.

Total integrated PF is  $5.59 \times 10^{10} \text{ mW m}^{-2} \text{ km}$ .

- 35% of PF enters the BPS
- 37% of PF enters the open field line regions (polar cap, void, mantle, cuspl)
- 8% of PF enters the LLBL
- 10% of PF enters the CPS

*These results are not reflected in the empirical models used for energy input to the GCMs!*

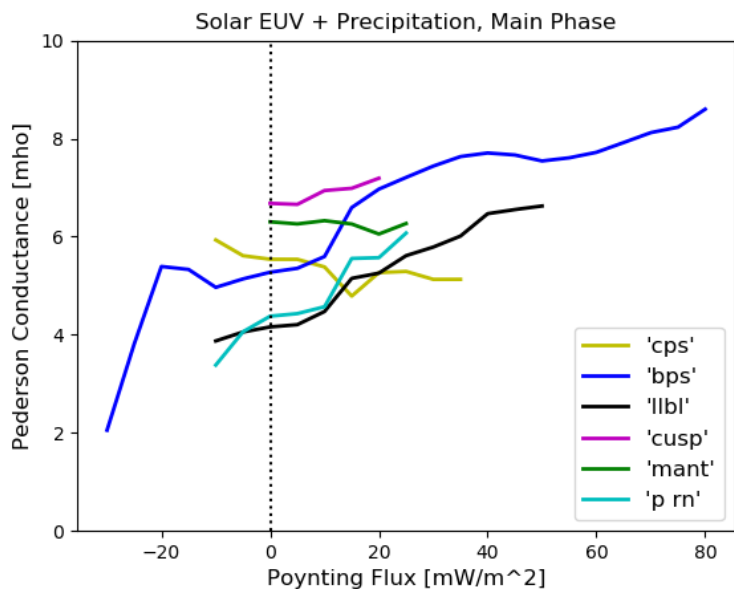
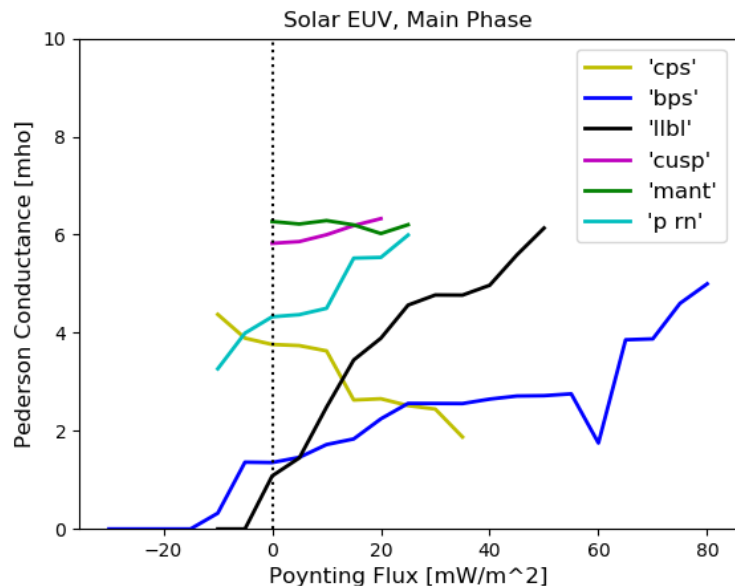
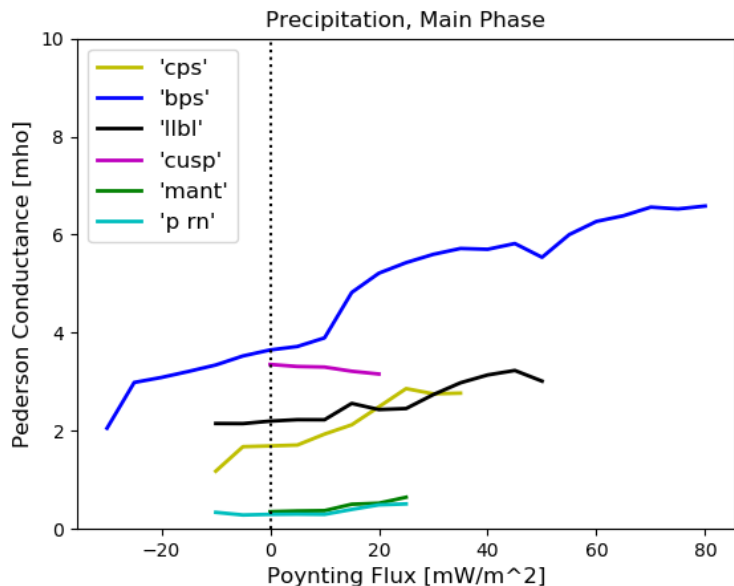
## Relation between Poynting flux and Pedersen conductance



On the dayside, conductance is dominated by solar irradiance which is positively correlated with PF.

On the nightside, there is a positive correlation between PF and conductance up to PF of about 10 mW m<sup>-2</sup> and no correlation for higher values.

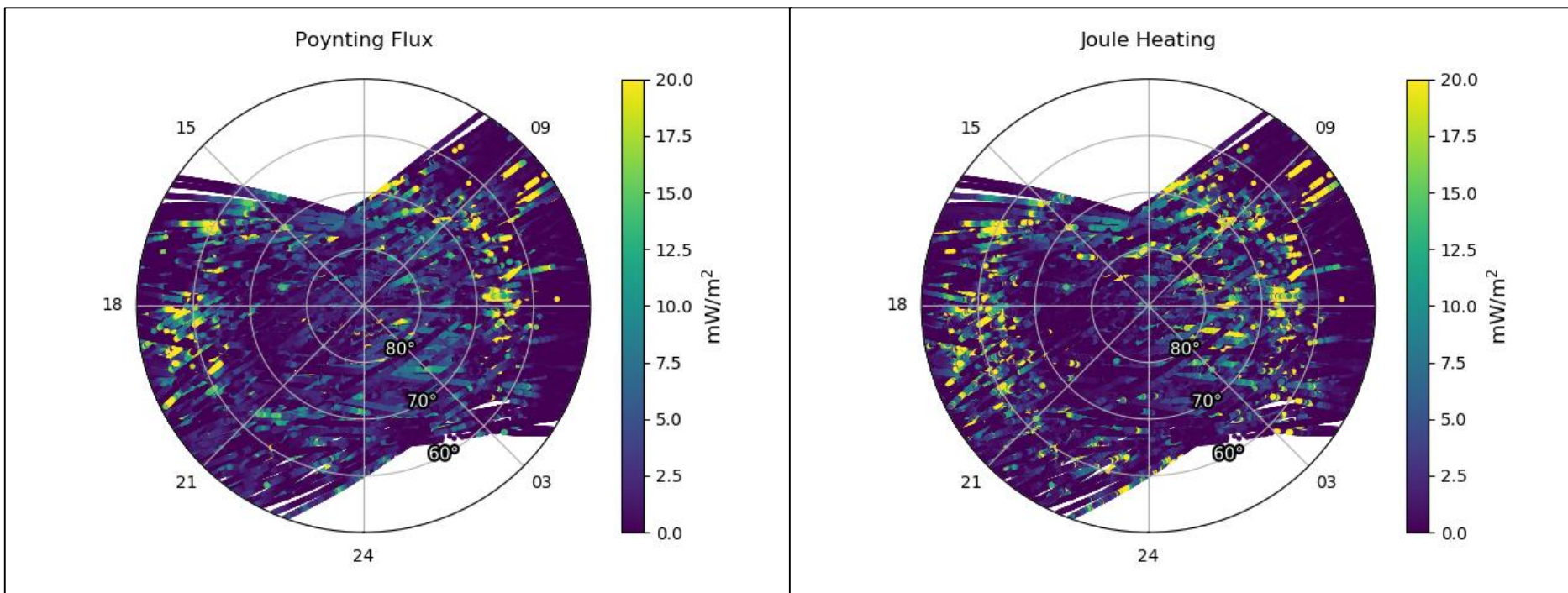
# Pedersen conductances vs PF for dayside regions



There is a positive correlation between Pedersen conductance and PF, due to dominance of solar contribution.

But the conductances are comparable for all regions, unlike the empirical models predictions.

Overplots of PF and JH for 44 storm main phases, for both hemispheres



$$S(mW m^{-2}) = \frac{E \times \delta B}{\mu_0}$$

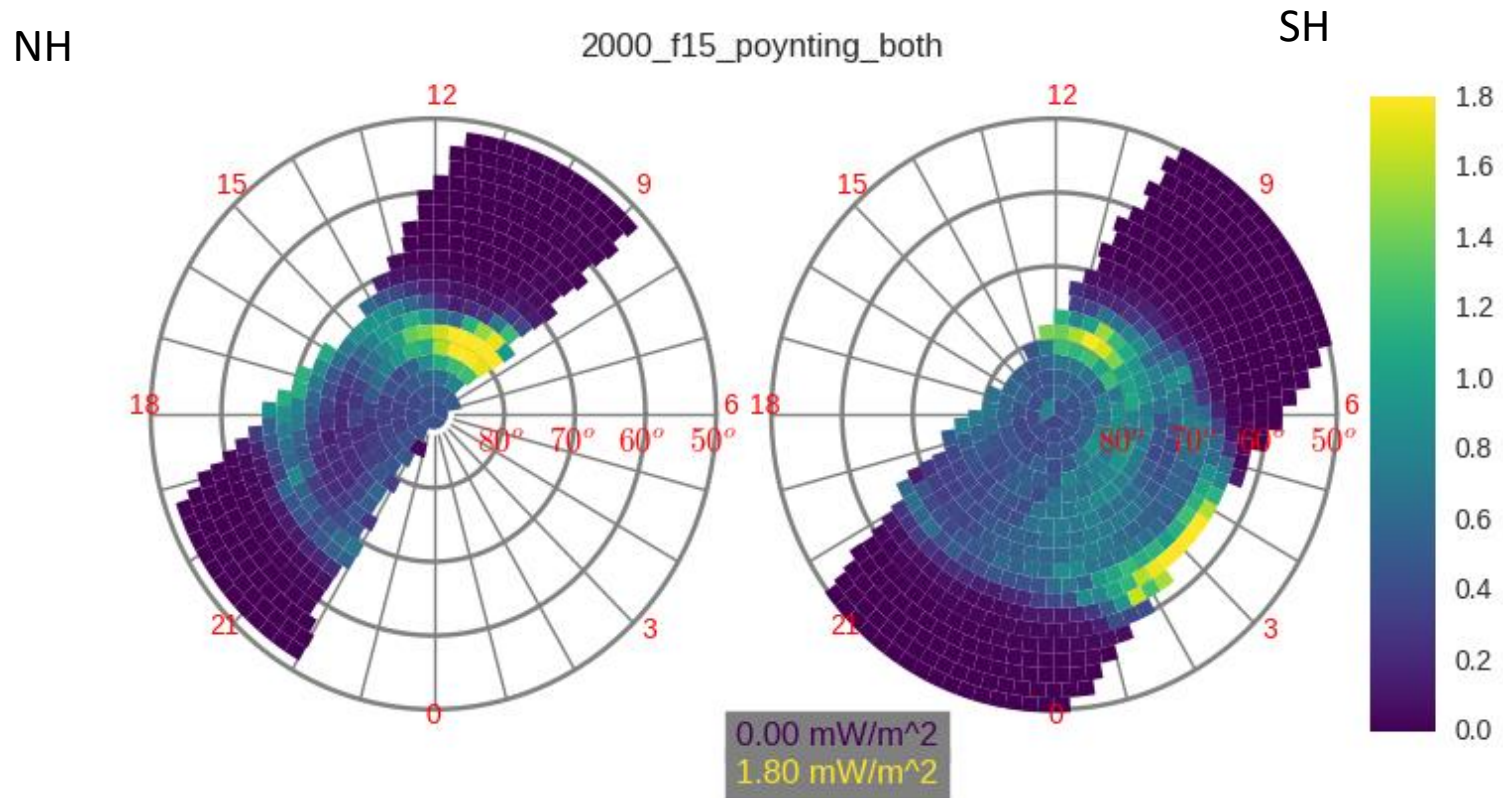
$$JH(mW m^{-2}) = \sigma_P E^2$$

There are differences in distribution of PF and JH [Thayer and Semeter, 2004].  
Dawn-dusk asymmetry is real and is seen in both hemispheres.



## Median Value Poynting Flux ( $S_{\parallel}$ )

### DMSP F15 Year 2000, Quality Flag = 1



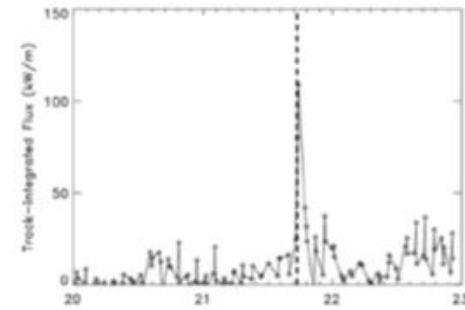
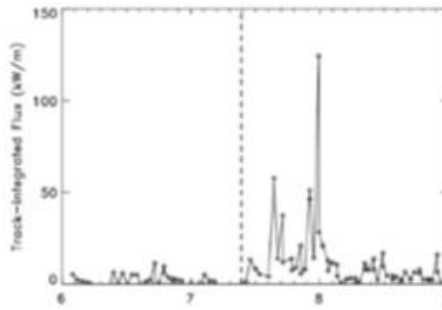
- Magnetic perturbations from de-trended, de-spiked data (Kilcommons et al. 2017)
- Electric field from Quality Level 1 ion drift and retarding potential analyzer data (de-trended)
- Plotted in magnetic coordinates in equal area bins

# Joule heating of neutrals at polar latitudes

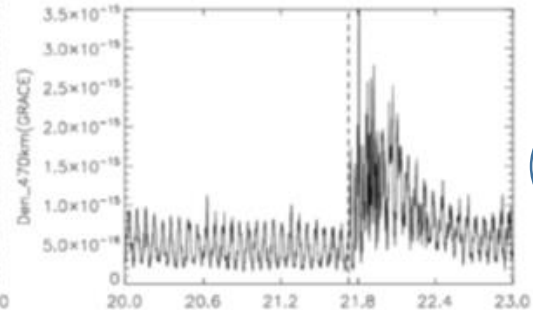
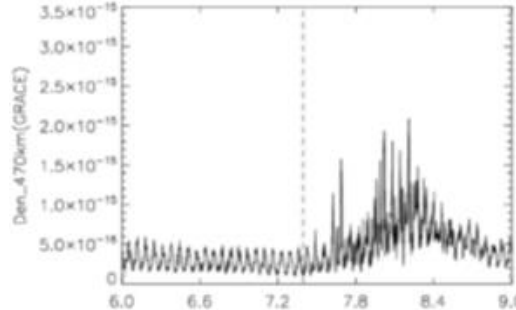
## Case Study: 2 magnetic storms, January 2005

Observations of Poynting flux from DMSP; neutral densities from GRACE, CHAMP; neutral temperatures from FPI at Resolute Bay [Huang, Y., et al., 2016].

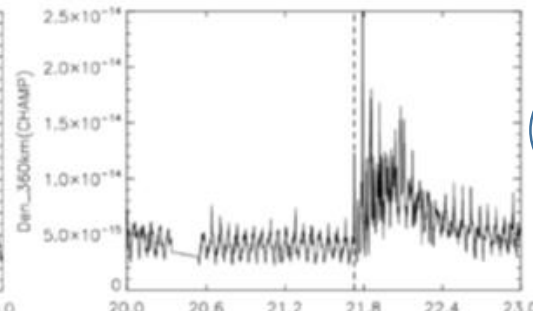
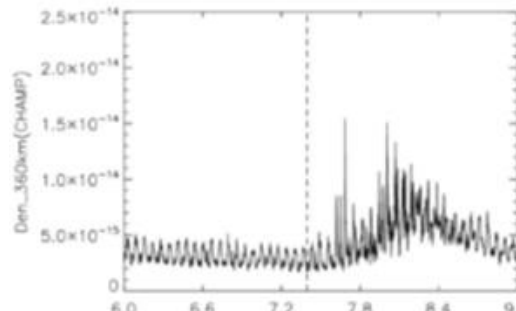
Maxima in PF coincide with increases in neutral densities at GRACE, CHAMP, and increase in neutral temperatures in FPI.



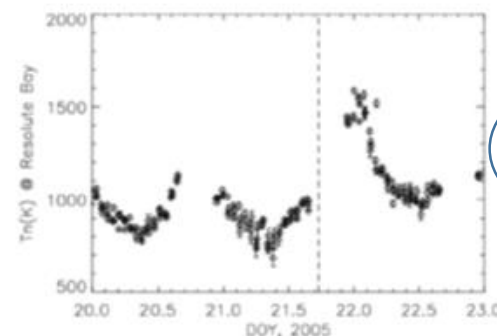
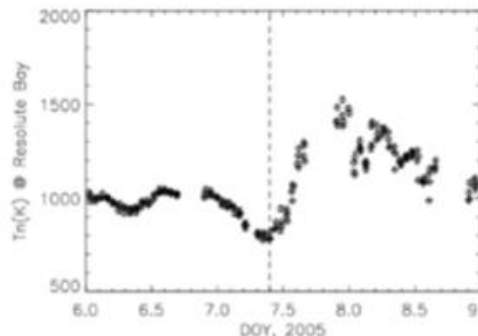
DMSP PF



GRACE  $N_n$

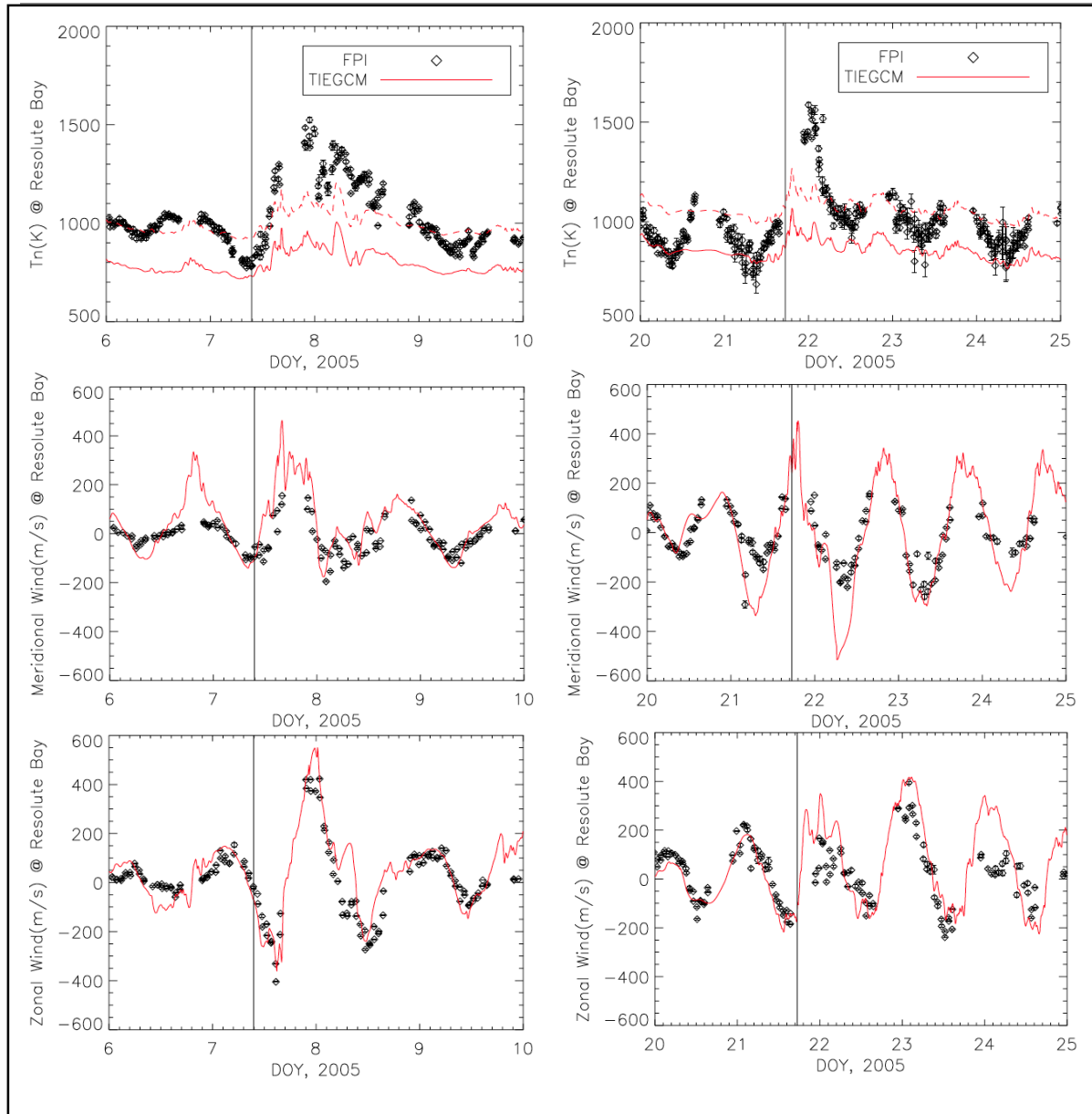


CHAMP  $N_n$



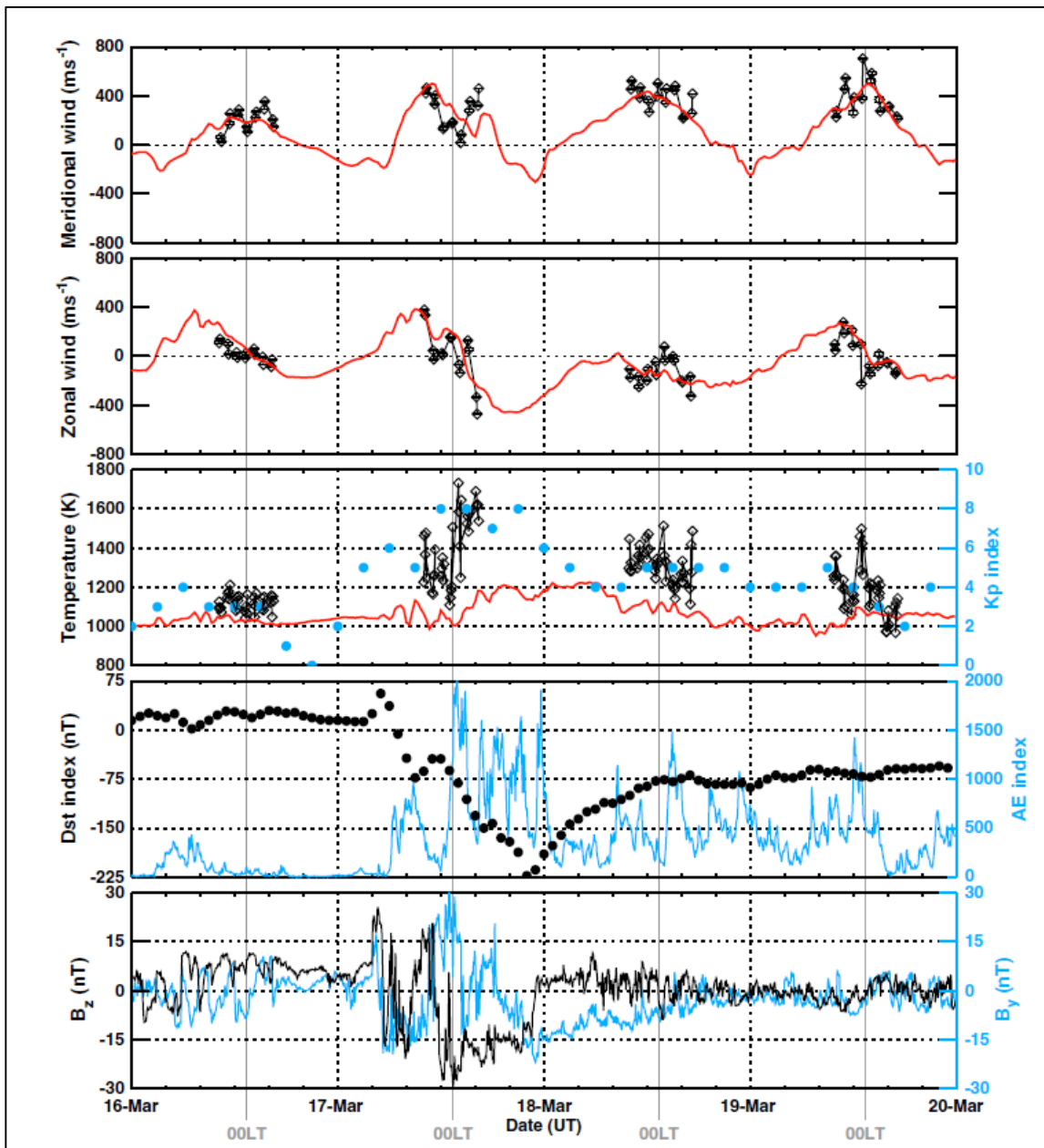
FPI  $T_n$

## Model predictions of neutral temperature



TIEGCM underestimates neutral heating substantially, but trends in  $T_n$  and neutral winds are in fairly good agreement with data [Huang, Y. et al., 2016].

# Model predictions of neutral temperature



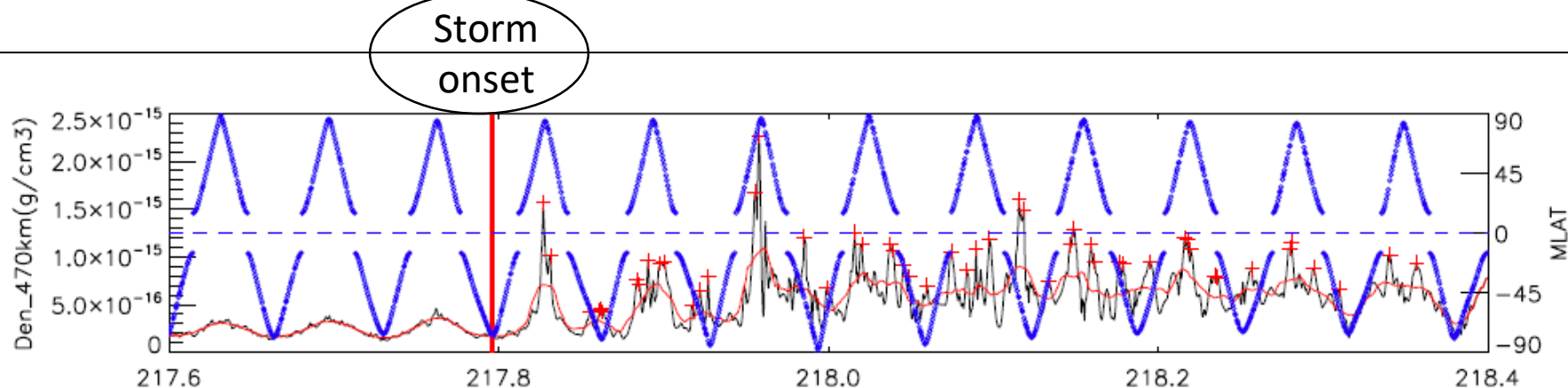
— TIEGCM  
 ◇ FPI observations

Similar results in separate study during magnetic storm, 17 March 2015, using FPI at Jang Bogo station, Antarctica [Lee et al., 2017].

Trends in TIEGCM agree with observations, but temperature increase is underestimated.

Joule heating of neutrals at polar latitudes is not captured by TIEGCM.

The effect of energy input is to heat ions which, in turn, can heat neutrals. The effect of heating the thermosphere is to expand and raise the thermosphere. This is observed at an orbiting satellite as an increase in measured density at a fixed altitude.



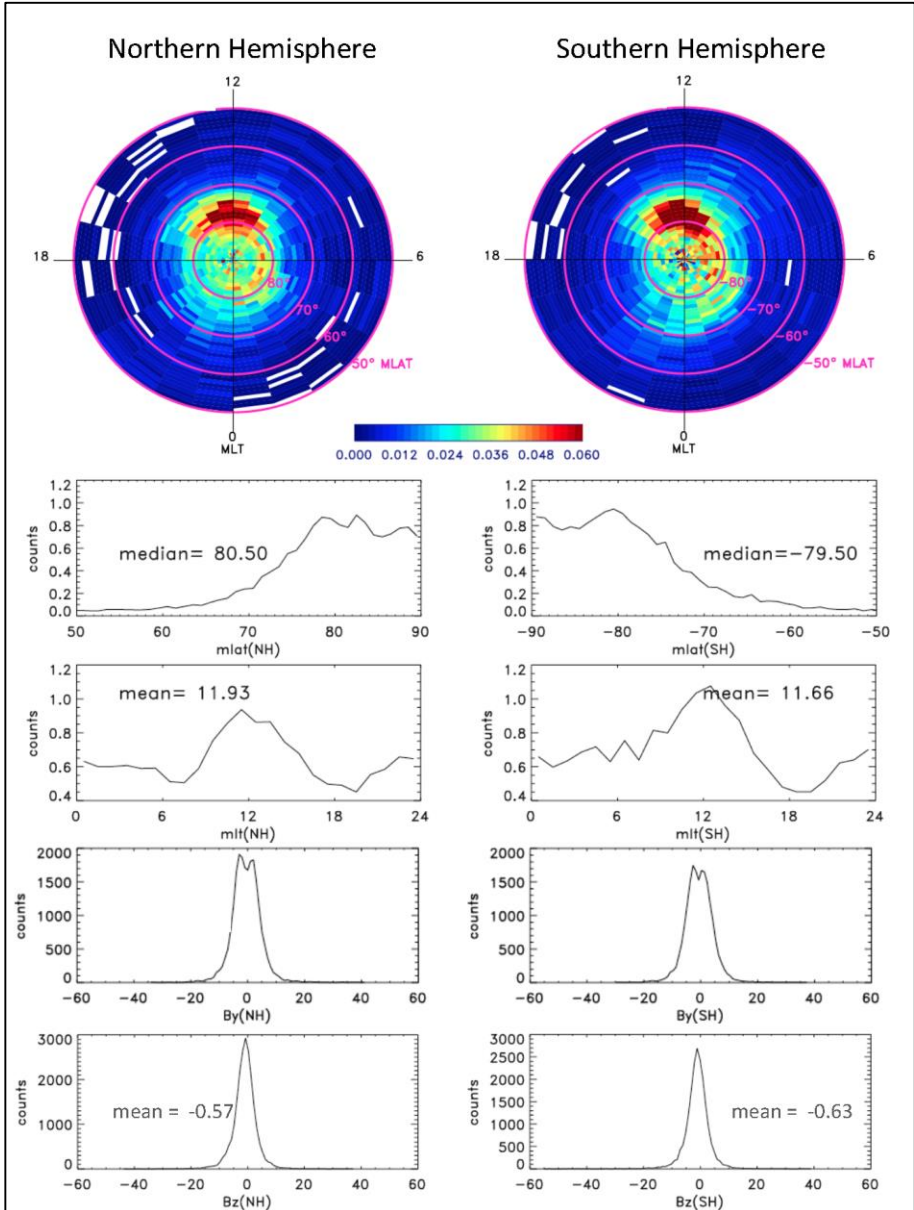
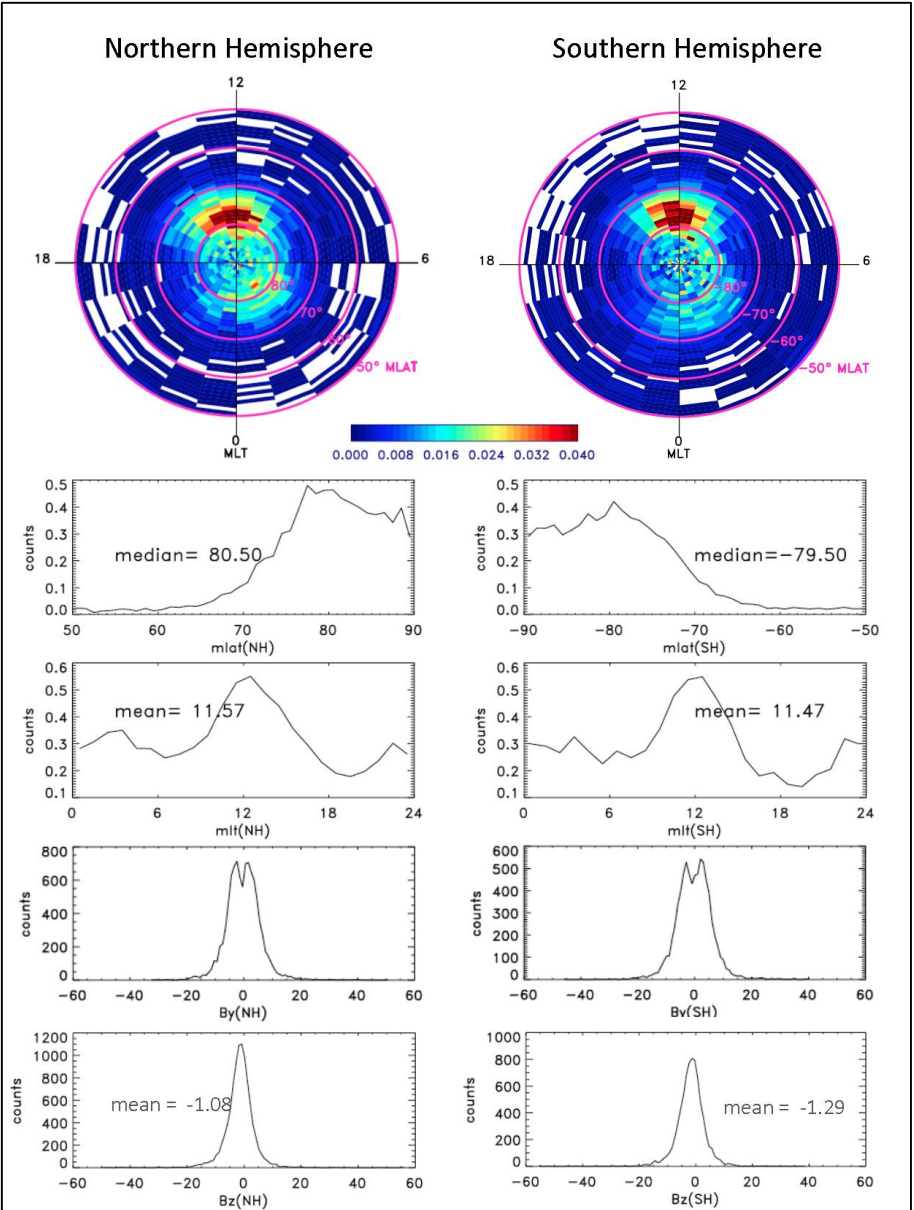
However Joule heating of neutrals creates Traveling Atmospheric Disturbances (TADs), gravity waves that propagate away from the heating location. These also appear as increases in measured density. Distinguishing between localized heating and TADs is challenging.

We have analyzed neutral densities measured indirectly by accelerometers on the CHAMP and GRACE spacecraft, from 2001-2010 (CHAMP) and 2002-2012 (GRACE). We extract the maxima by fitting a baseline to 90° of the orbit, defining the maxima as any point that is 30% above the baseline.



# Normalized neutral mass density maxima

CHAMP (left) 2001-2010; GRACE (right) 2002-2012 [Huang et al., 2017]



The CHAMP and GRACE results show the same trends:

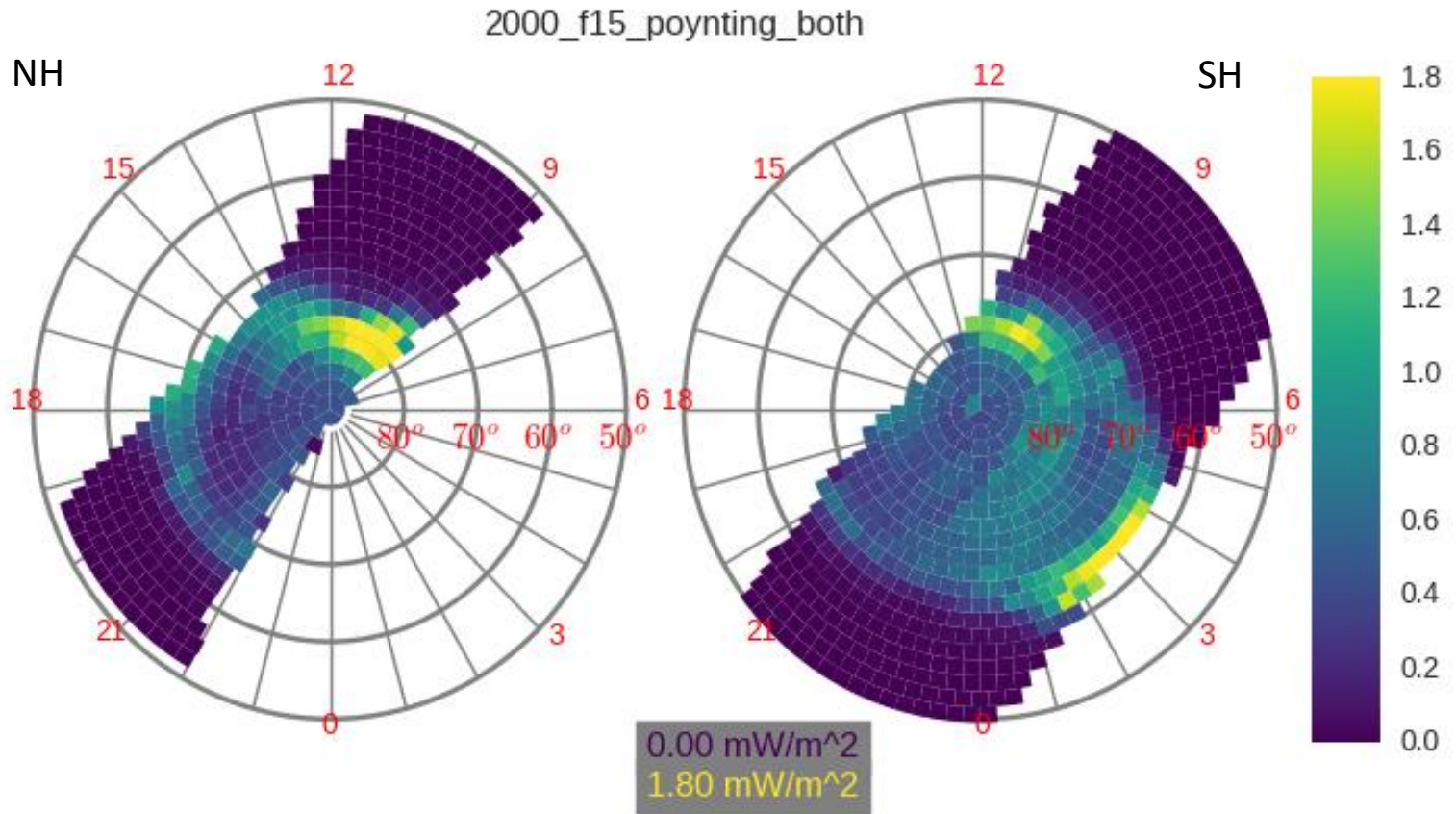
- Normalized neutral density maxima peak at  $\sim 80^\circ$  Mlat in both hemispheres.
- The width of this peak is around  $10^\circ$ , extent in MLT 2-3 hours.
- Location and size rule out the cusp which is less than  $1^\circ$  wide in latitude, and is typically located at  $73-77^\circ$  Mlat [Newell et al., 2005].
- Analysis of individual storm periods shows that some of the maxima are associated with field-aligned currents (FACs), indicative of localized heating; but some maxima are not. The majority of FACs are not associated with neutral density maxima.
- There is no sign of a maximum in occurrence at auroral latitudes/BPS.

Similar results have been reported by Lühr et al. (2004); Liu et al. (2010); Kervalishvili and Lühr (2013). There is no consensus on how to separate localized heating from TADs in the observations.

*What is the cause of the high-latitude hot spot in neutral density maxima?*



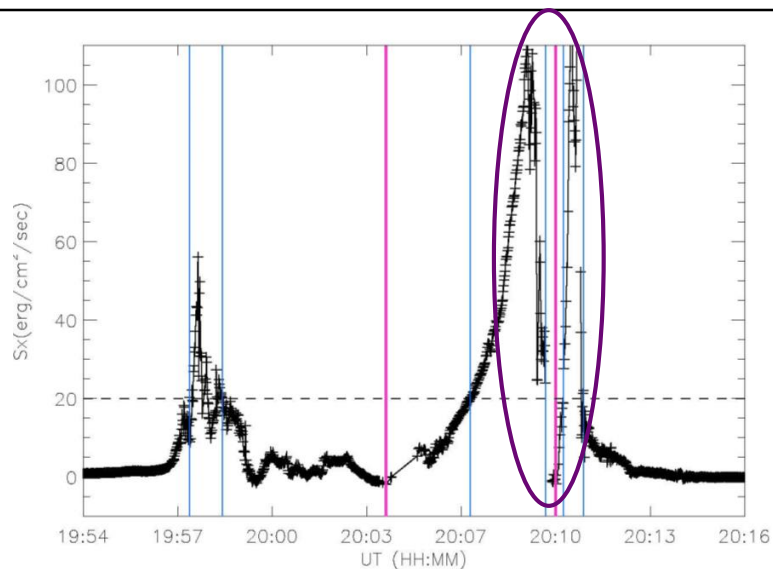
## Poynting flux again!



The average observed PF shows a maximum at approximately the same latitude and local time as the neutral density maximum. The resemblance is striking.

## Outline:

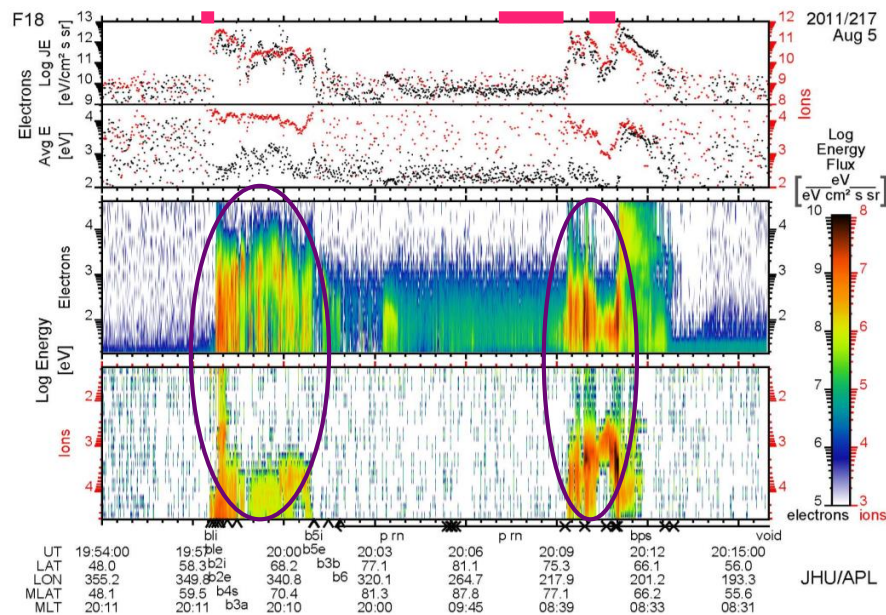
- Introduction
- Physics-based models
  - Solar wind drivers
- Observations of energy input
  - Poynting flux and Joule heat
- Observations of energy dissipation
  - Particle precipitation and conductance
  - Heating of neutrals
- **Outstanding challenges**
  - **Scale sizes, variability**
  - **Geoeffectiveness**



The observed high latitude PF and particle precipitation are highly structured.

What effect does this have on the IT system?

Studies indicate that the perturbations in  $E$  and  $B$  fields contribute to total Joule heating [Codrescu et al., 1995, 2008; Deng et al., 2007, 2009; Fedrizzi et al., 2012; Matsuo et al., 2003, and others].



Use of smoothed, averaged climatology for the high-latitude drivers can lead to underestimates of energy input to the IT system.

# Variability of E and B fields

Variability of E-field:  $E = \underline{E_L} + \underline{E_S}$   
 Large-scale variation Small-scale variation

Variability of B-field:  $\Delta B = \underline{\Delta B_L} + \underline{\Delta B_S}$   
 Large-scale variation Small-scale variation

Energy input:  $PF = \frac{1}{\mu_0} (E \times \Delta B) = \frac{1}{\mu_0} (E_L \times \Delta B_L + \underline{E_L \times \Delta B_S + E_S \times \Delta B_L + E_S \times \Delta B_S})$   
 (Poynting flux)

Small-scale variability contribution to PF:  $\frac{E_L \times \Delta B_S + E_S \times \Delta B_L + E_S \times \Delta B_S}{E \times \Delta B}$

Energy Dissipation:  $JH = \sigma_P E^2 = \sigma_P (E_L^2 + \underline{2E_L E_S} + E_S^2)$   
 (Joule heating)

Small-scale variability contribution to JH:  $\frac{2E_L E_S + E_S^2}{E^2}$  [Huang, Y., et al., AGU 2016]

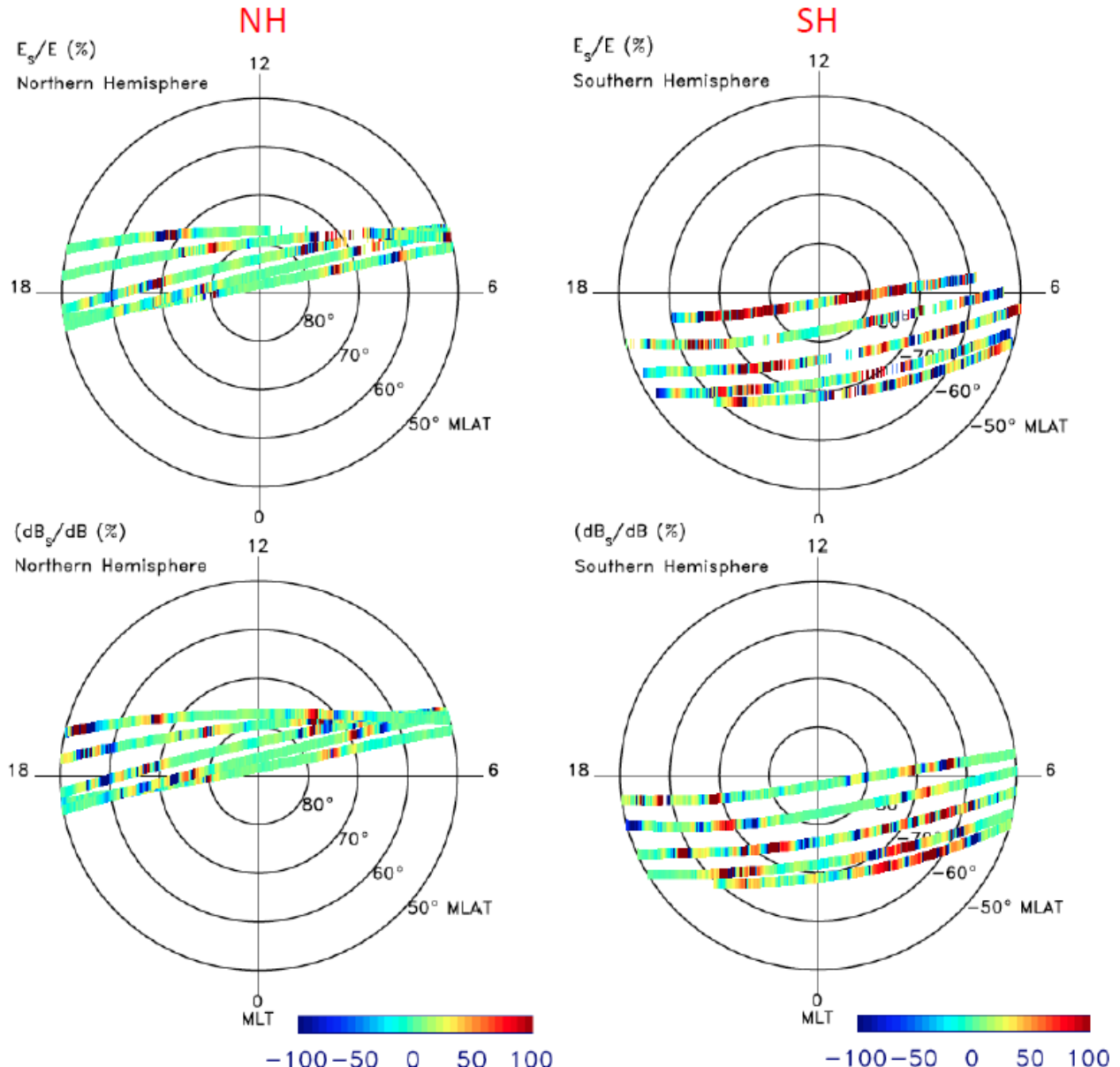
# Aug 2011 storm main phase (F16)

$E_s/E$  (%)

Median magnitude of change ~ 15%

$\Delta B_s/\Delta B$  (%)

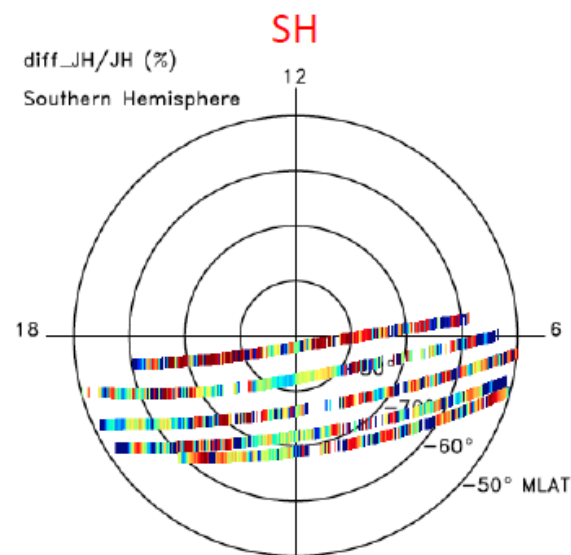
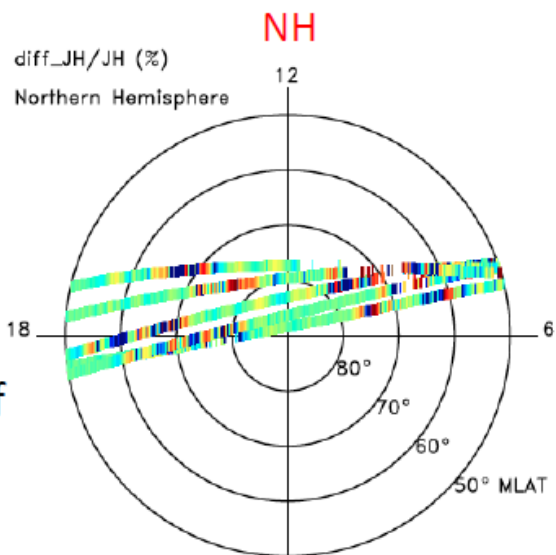
Median magnitude of change ~ 20%



# Aug 2011 storm main phase (F16)

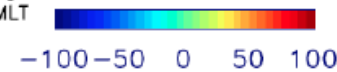
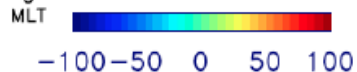
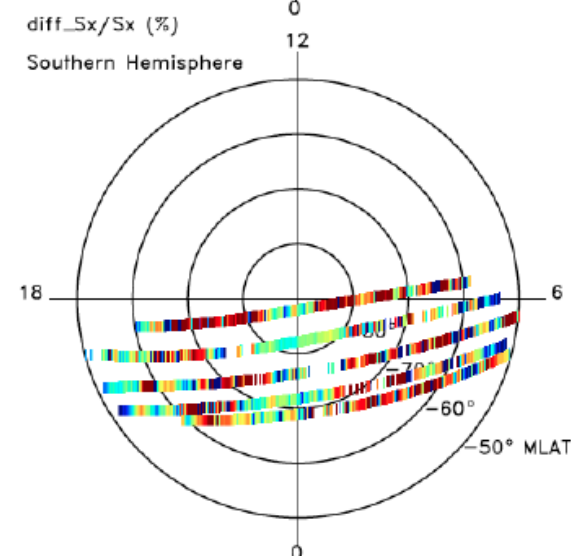
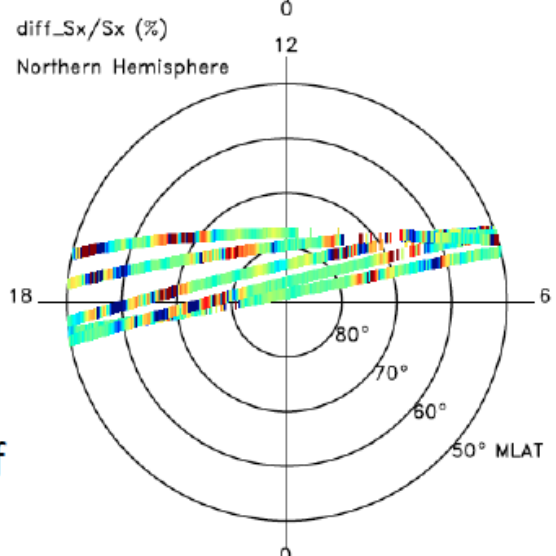
Contribution from small-scale variability to JH (%)

Median magnitude of change ~ 27%



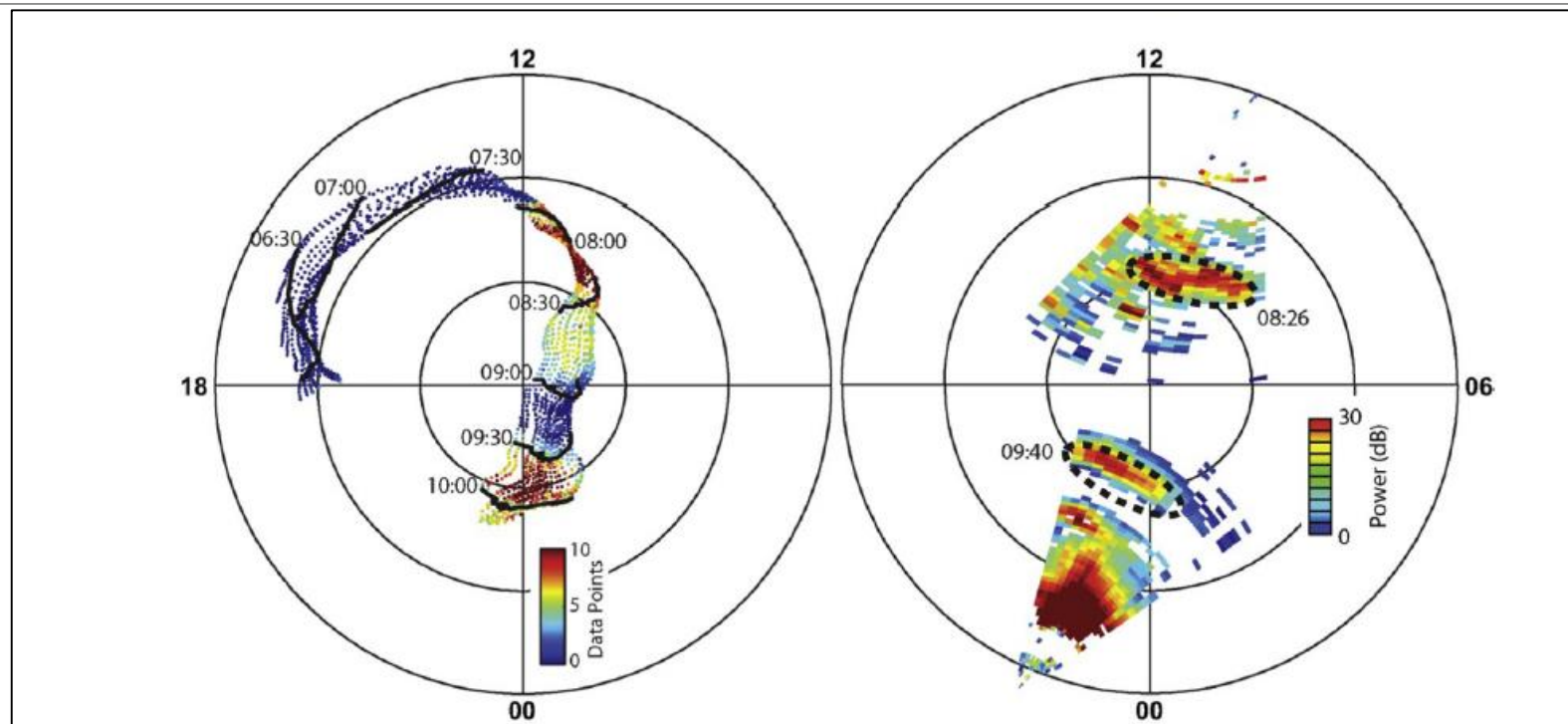
Contribution from small-scale variability To PF (%)

Median magnitude of change ~ 35%



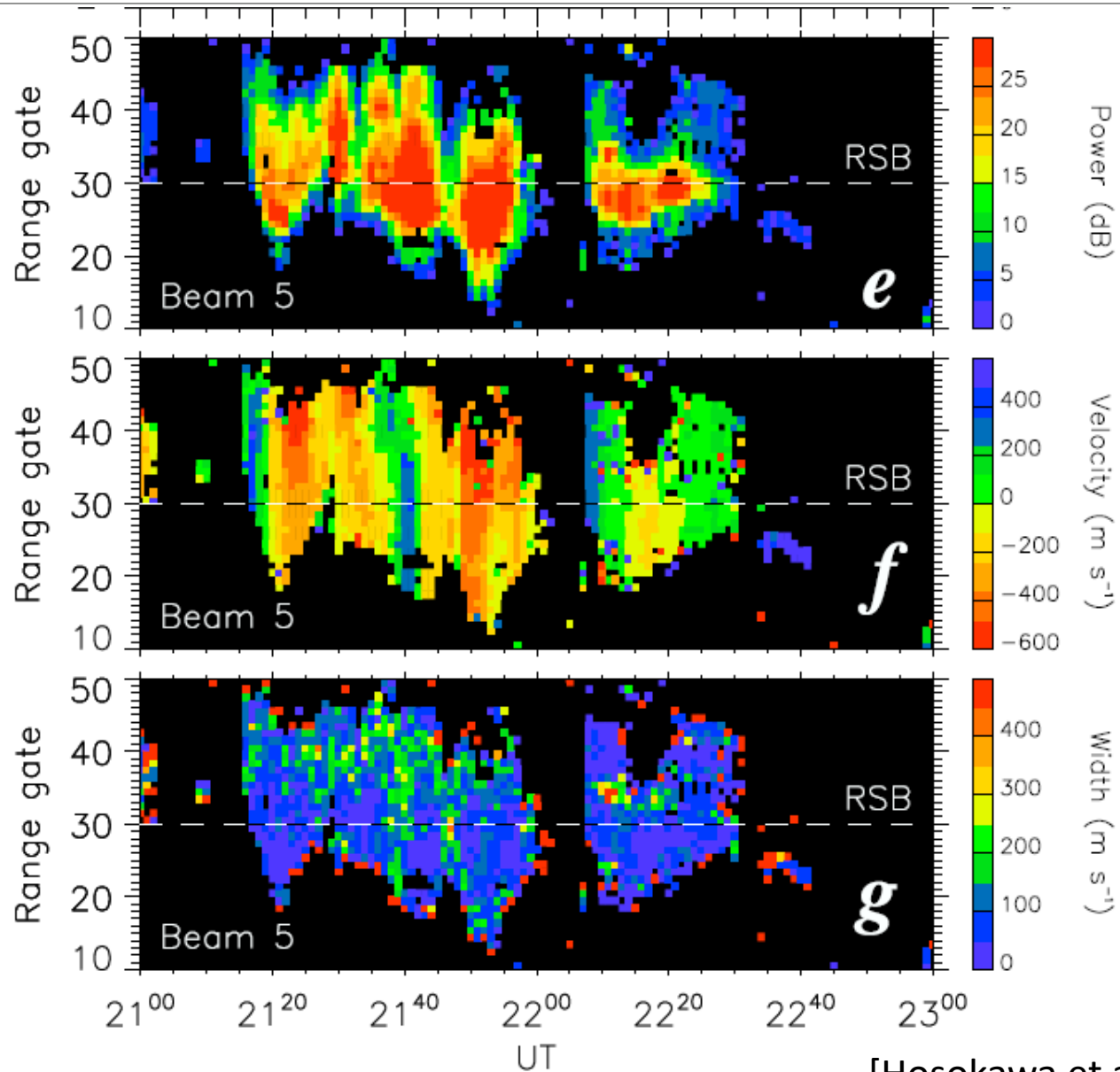


## Digression: Polar cap patches



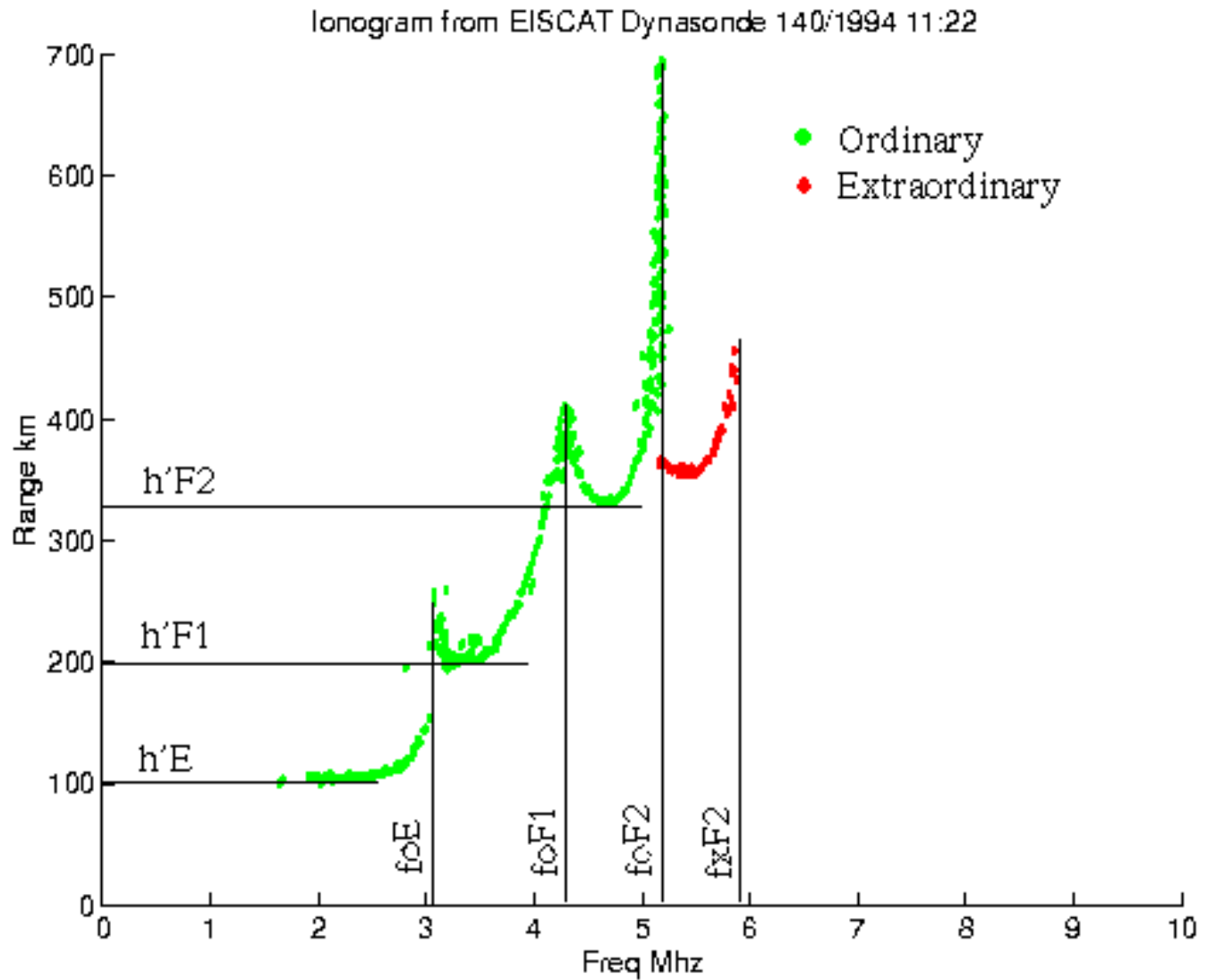
[Moen et al., 2012]

- Polar cap patches are regions of cold plasma, 100s km in extent, with F-region densities twice the ambient polar cap density.
- Patches drift across the polar cap, typically from day to night, at speeds of 1-2 km s<sup>-1</sup>.
- Within the patches, irregularities at scales from meters to km disrupt electromagnetic wave propagation from HF to GNSS frequencies.



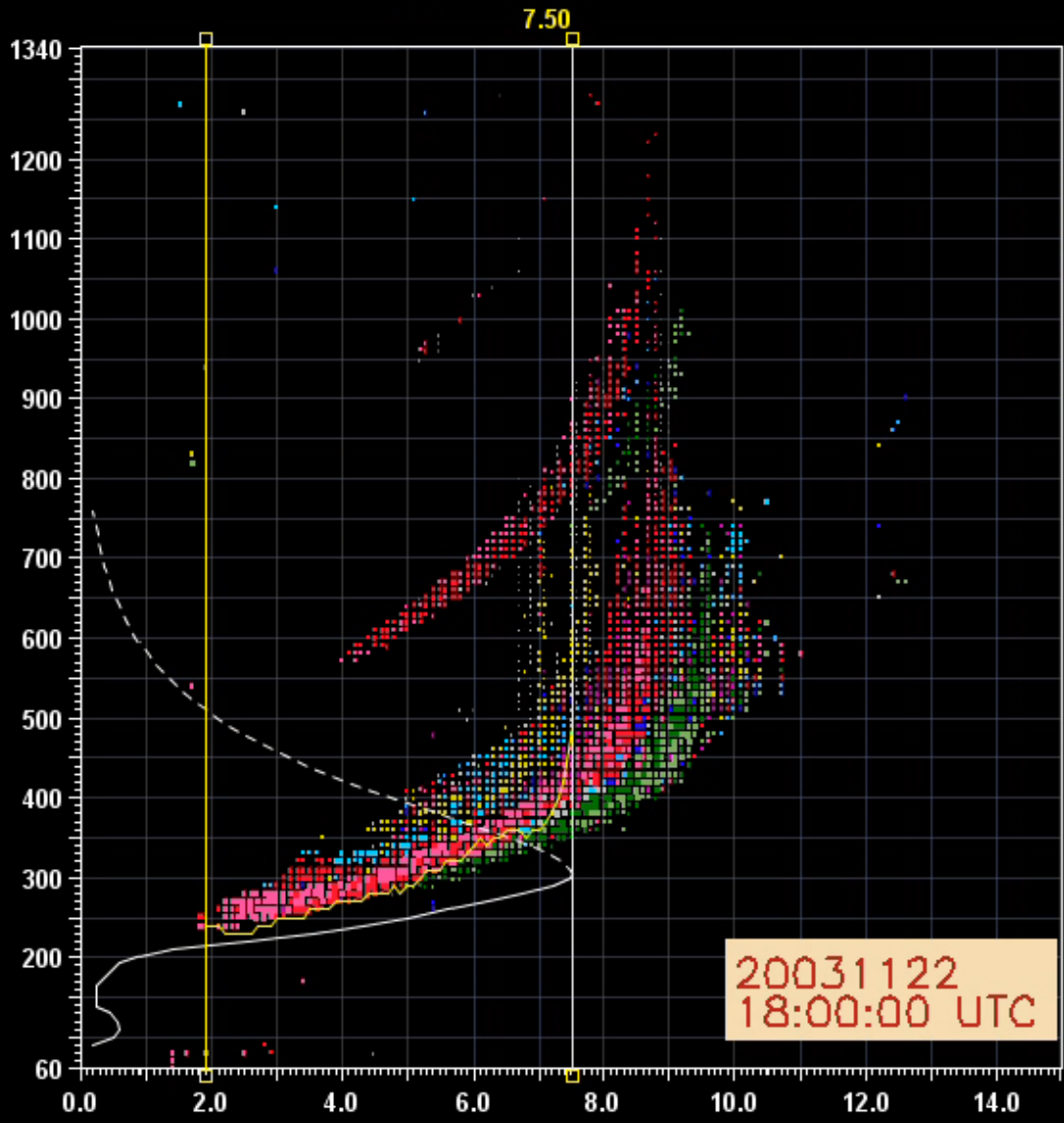
[Hosokawa et al., 2009]

# Ionograms



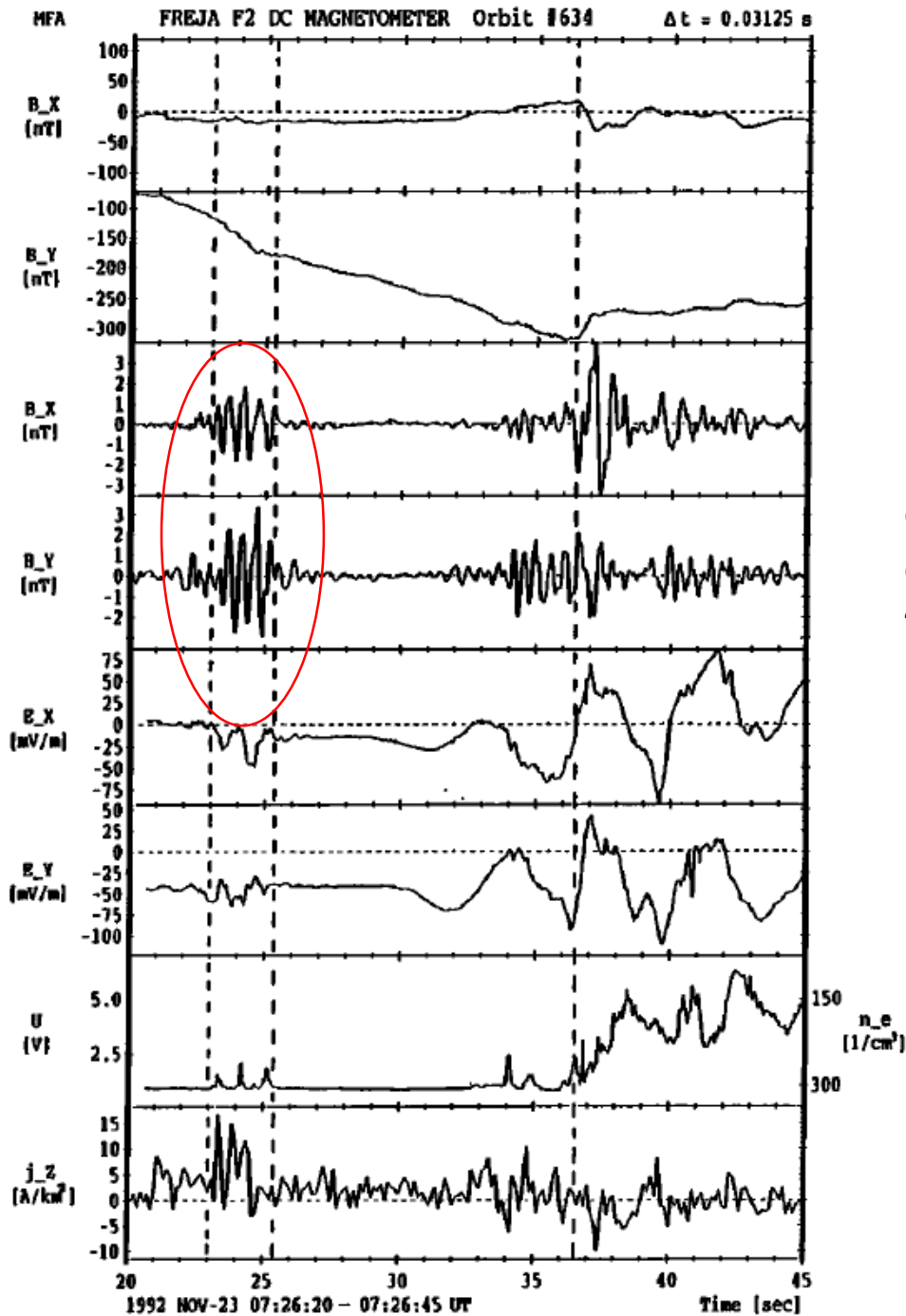
Qaanaaq, THJ77

2003.11.22 (326) 18:00:05.000 SI\_  
C-level 11



NoVal
ESE
WNW
WSW
V-
V+
Vx-
Vx+
S
N
ENE

## Small scale variability in magnetic field measurements



Magnetic fluctuations from Freja (altitude of 1600 km) [Lühr et al., 1982]. Scale size of fluctuations mapped to the ionosphere  $\sim 1.5$  km

### 1. What are the geoeffective time/length scales for energy input and dissipation?

These need to be determined before we modify models to represent solar wind driving of IT more realistically.

We assume that geoeffectiveness will vary with the processes being considered, e.g. electrodynamic coupling is generally assumed to be fast (how fast?), but neutral heating is assumed to be slow (how slow?). HF waves are affected by decameter structure in the ionosphere, but VLF is not. Geoeffectiveness needs to be quantified.

### 2. How can we capture the geoeffective drivers at high latitudes?

Most attempts to include small-scale variability have been based on empirical approaches which remove much of the variability. Assimilation requires dense data sources which are sparse at high latitudes. We need a different approach to this problem.

### 3. Are small scales coupled to the large scales?

This fundamental question has not been answered yet. As we go to smaller and smaller scales, at what point does MHD break down, and kinetic theory become the relevant approach? How geoeffective are small-scale effects, and are these linked to larger scales?



- The high-latitude IT system is highly dynamic in space and time.
- It is also a region where data are sparse.
- Physics-based models do not perform well in validation studies of either Joule heat or neutral density during magnetic activity.
- The most widely used high-latitude drivers for GCMs are empirical. These cannot capture dynamics.
- ***The high-latitude IT system remains a challenging area of research!***